



QCD Phase Transitions at finite temperature and densities within FRG approach

Wei-jie Fu

Dalian University of Technology

666. WE-Heraeus-Seminar on “From Correlation Functions to QCD
Phenomenology”

April 3-6, 2018, Bad Honnef, Germany

Collaborators:

fQCD collaboration (J. Braun, L. Corell, A. Cyrol, WF, M. Leonhardt, M. Mitter,
J.M. Pawłowski, M. Pospiech, F. Rennecke, N. Strodthoff, N. Wink), Bernd-
Jochen Schaefer, Rui Wen, Chuang Huang, Ke-Xin Sun et al.

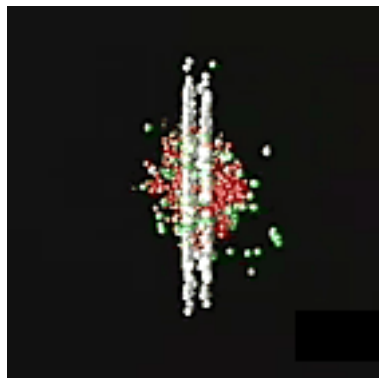
Outline

- * **Introduction**
- * **Baryon number fluctuations, probability distribution in low energy effective models**
- * **Quantum fluctuations of gluons and QCD phase transition**
- * **Summary and outlook**

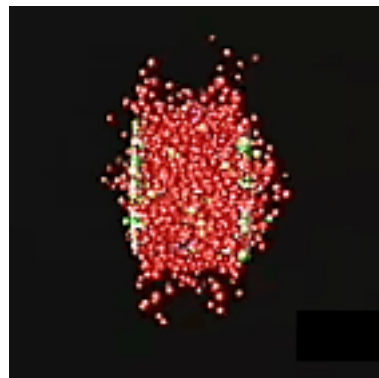
Heavy-ion collision



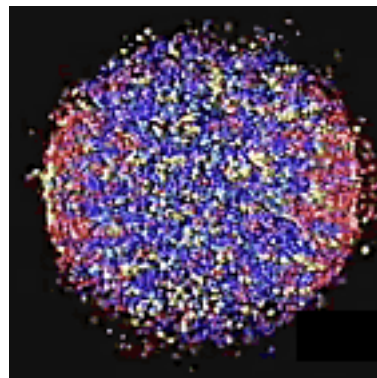
Ions about to collide



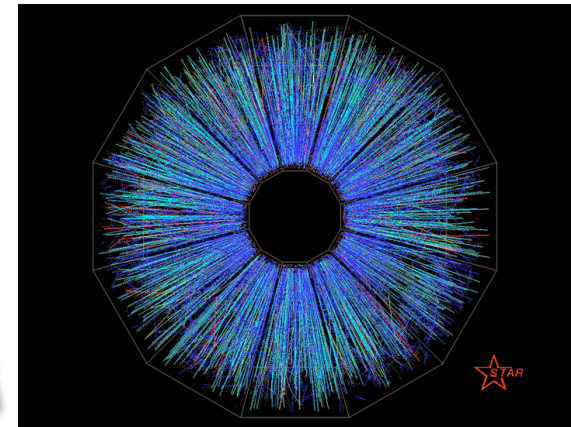
Ion collision



Plasma formation



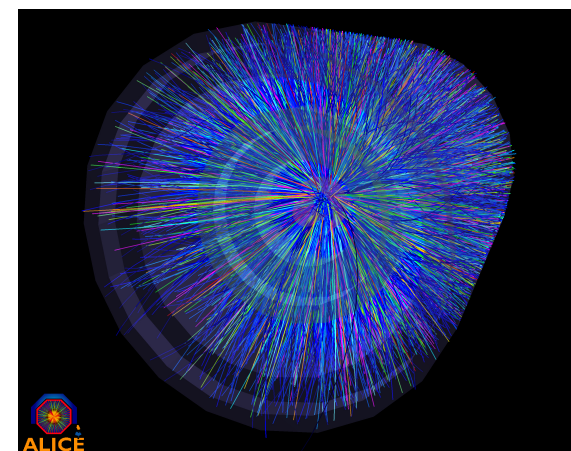
Freeze out



STAR

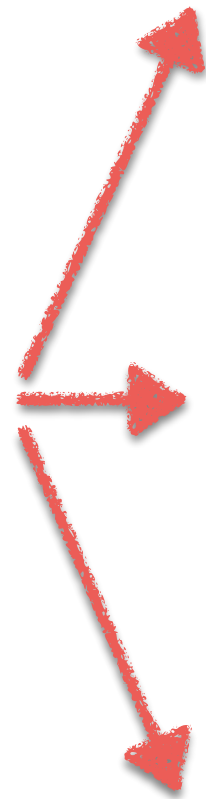


PHENIX

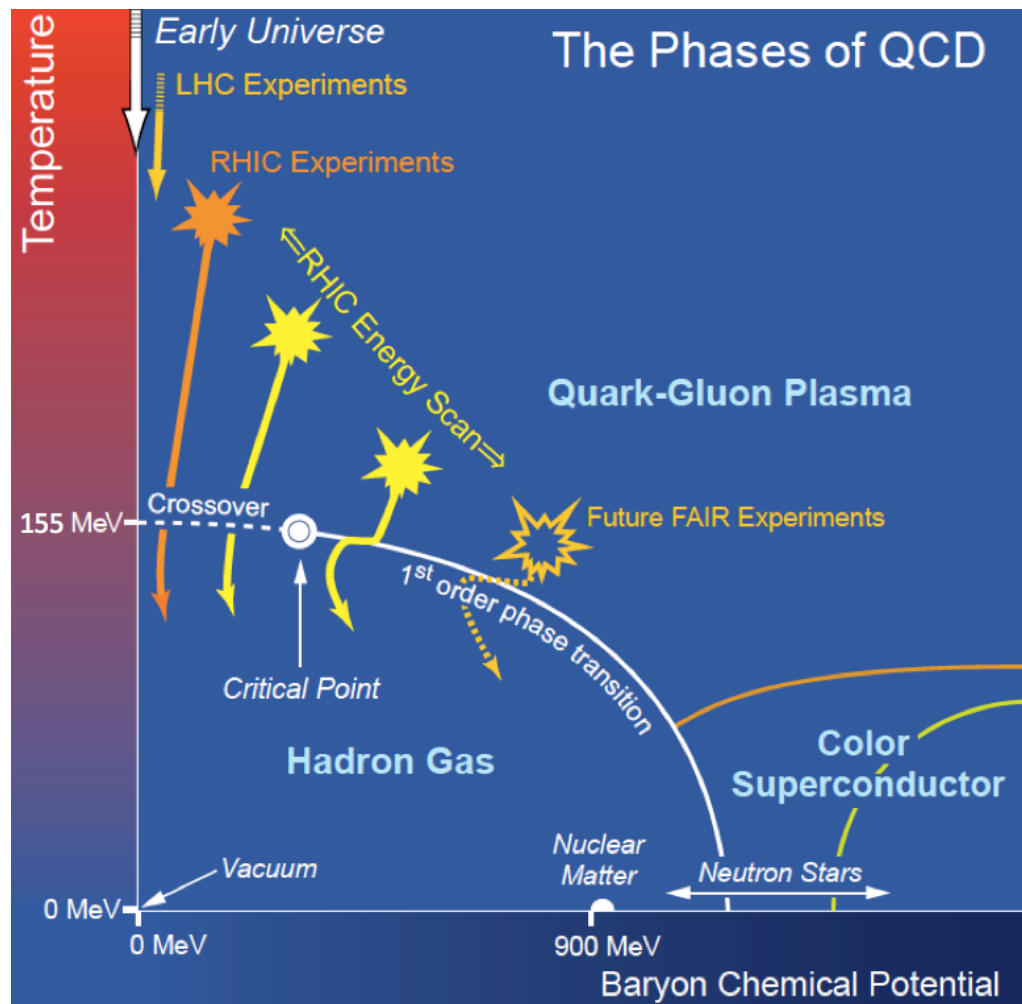


ALICE

What we see

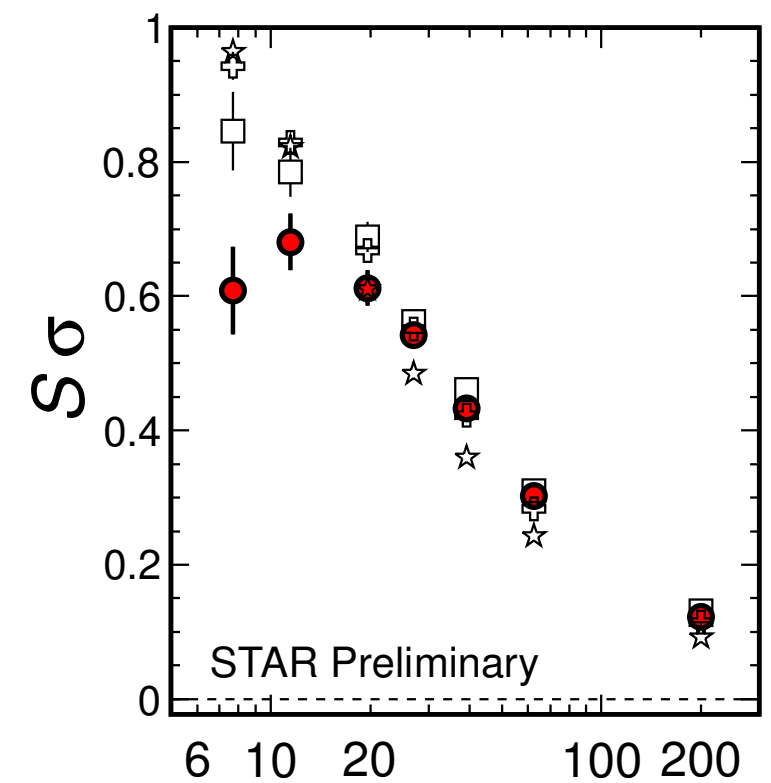
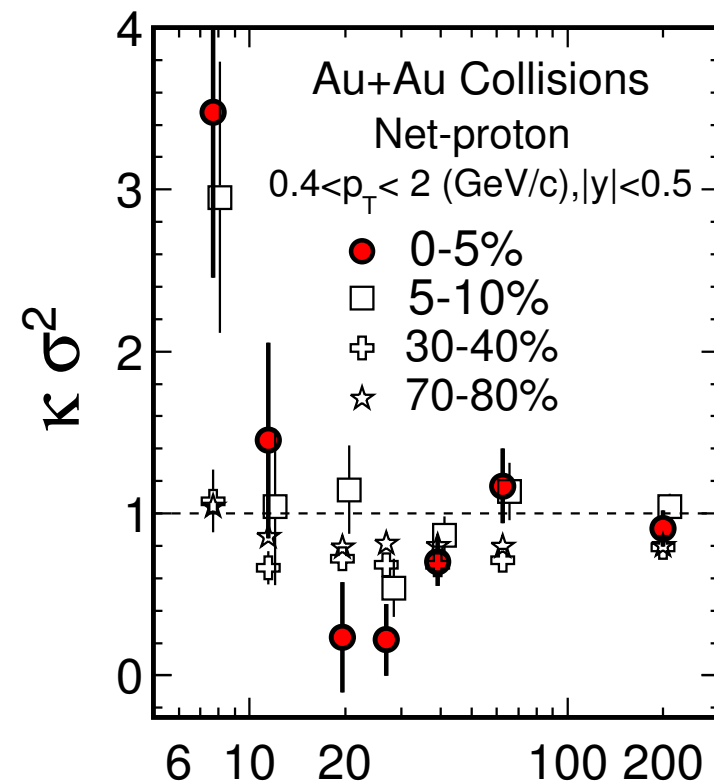


QCD Phase Structure



The Hot QCD White Paper (2015)

RHIC:



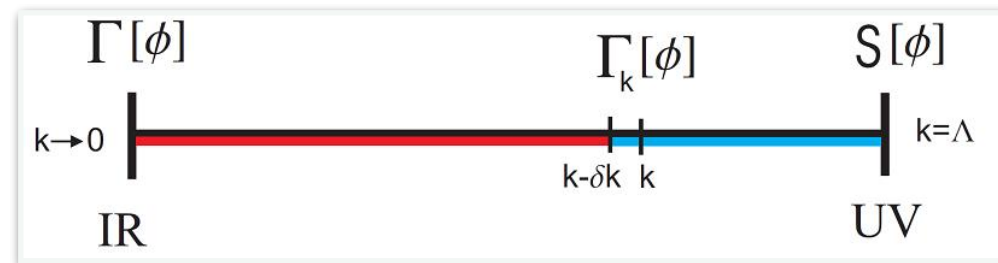
Colliding Energy $\sqrt{s_{NN}}$ (GeV)

X.Luo (STAR), PoS CPOD2014, 019 (2014)

Quantum Fluctuations with FRG

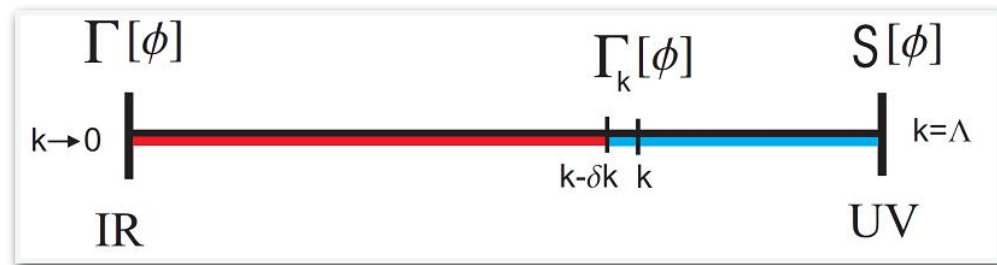
Quantum Fluctuations with FRG

FRG



Quantum Fluctuations with FRG

FRG

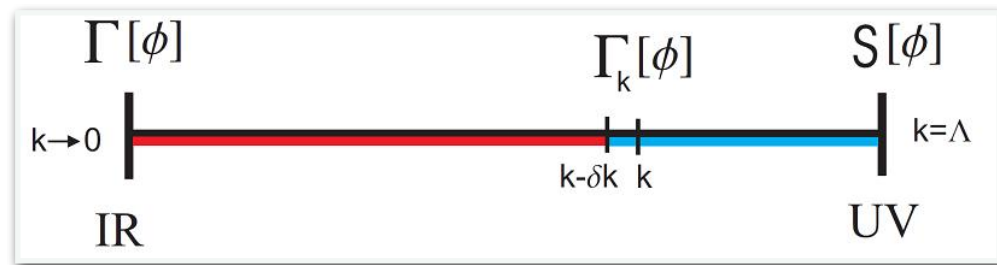


$$\partial_t \Gamma_k = \frac{1}{2} \left(\text{Diagram 1} - \text{Diagram 2} - \text{Diagram 3} + \frac{1}{2} \text{Diagram 4} \right)$$

The equation shows four Feynman diagrams representing the flow of the effective action. Each diagram has a top vertex (circle with an 'X') and a bottom vertex (black dot).
1. A solid loop with a wavy internal line.
2. A dashed loop with a wavy internal line.
3. A solid loop with a solid internal line.
4. A dashed loop with a dashed internal line.

Quantum Fluctuations with FRG

FRG



$$\partial_t \Gamma_k = \frac{1}{2} \left[\text{Diagram 1} - \text{Diagram 2} \right] - \text{Diagram 3} + \frac{1}{2} \text{Diagram 4}$$

Diagram 1: A loop with a wavy line (glue sector) and a solid line, with a cross in a circle at the top and a dot at the bottom.

Diagram 2: A loop with a dashed line and a solid line, with a cross in a circle at the top and a dot at the bottom.

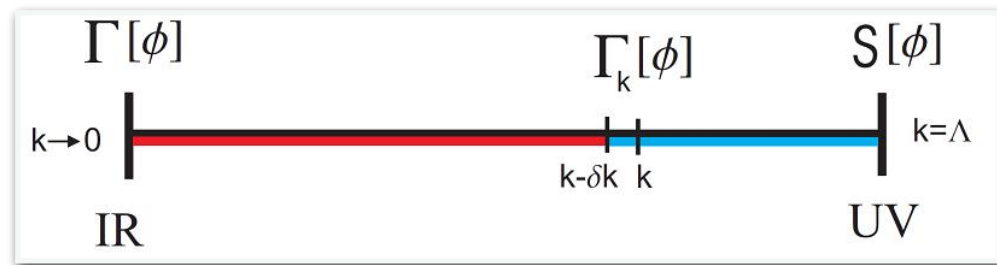
Diagram 3: A loop with a solid line, with a cross in a circle at the top and a dot at the bottom.

Diagram 4: A loop with a dashed line, with a cross in a circle at the top and a dot at the bottom.

A red arrow points from the text "glue sector" to the wavy line in Diagram 1.

Quantum Fluctuations with FRG

FRG



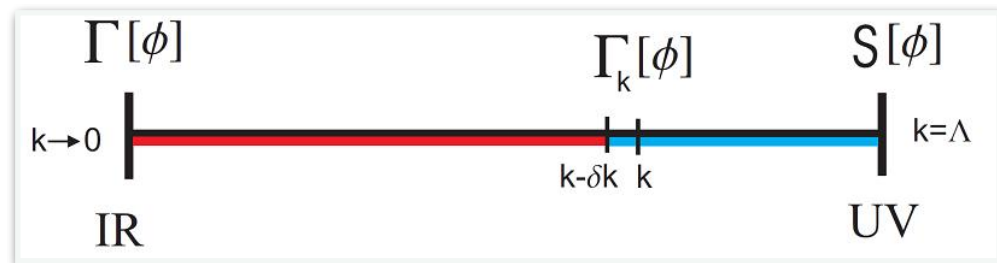
$$\partial_t \Gamma_k = \frac{1}{2} \left(\text{Diagram 1} - \text{Diagram 2} - \text{Diagram 3} + \frac{1}{2} \text{Diagram 4} \right)$$

The equation shows the flow of the effective action Γ_k with respect to the renormalization scale t . The right-hand side consists of four diagrams, each representing a quantum fluctuation:

- Diagram 1:** A loop with a wavy line (representing a ghost) and a solid line (representing a fermion). Both lines have a cross in a circle at their top and bottom vertices.
- Diagram 2:** A loop with a dashed line (representing a ghost) and a solid line (representing a fermion). Both lines have a cross in a circle at their top and bottom vertices.
- Diagram 3:** A loop with a solid line (representing a fermion) and a dashed line (representing a ghost). Both lines have a cross in a circle at their top and bottom vertices.
- Diagram 4:** A loop with a dashed line (representing a ghost) and a dashed line (representing a ghost). Both lines have a cross in a circle at their top and bottom vertices.

Quantum Fluctuations with FRG

FRG



Matter part, effective models

2 flavor

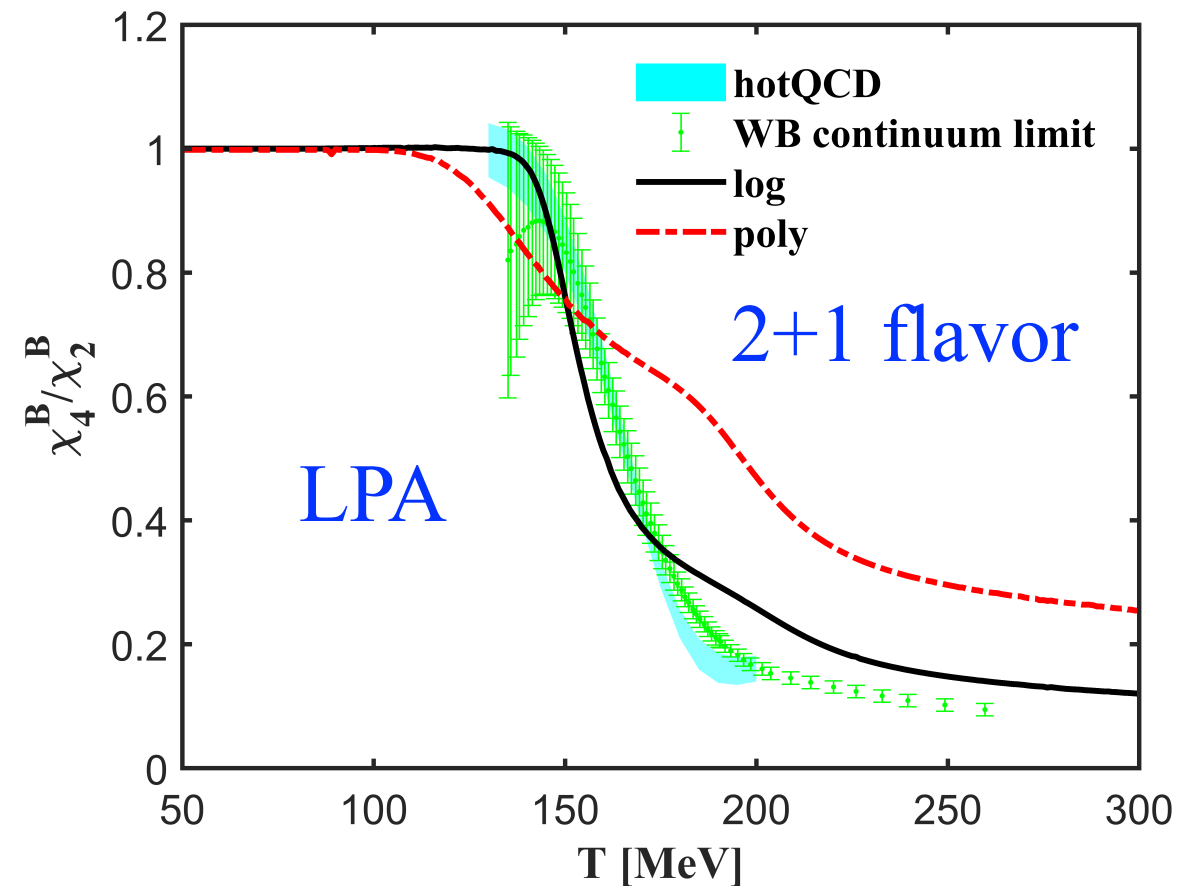
$$\Gamma_k = \int_x \left\{ Z_{q,k} \bar{q} (\gamma_\mu \partial_\mu - \gamma_0 \mu) q + \frac{1}{2} Z_{\phi,k} (\partial_\mu \phi)^2 + h_k \bar{q} \left(T^0 \sigma + i \gamma_5 \vec{T} \cdot \vec{\pi} \right) q + V_k(\rho) - c\sigma \right\} + \dots$$

$$\partial_t \Gamma_k = \frac{1}{2} \left(\text{Diagram 1} - \text{Diagram 2} - \text{Diagram 3} + \frac{1}{2} \text{Diagram 4} \right)$$

2+1 flavor

$$\Gamma_k = \int_x \left\{ \bar{q} [\gamma_\mu \partial_\mu - \gamma_0 (\mu + ig A_0)] q + V_{\text{glue}}(L, \bar{L}) + \text{tr}(\partial_\mu \Sigma \cdot \partial_\mu \Sigma^\dagger) + i \bar{q} h_k \cdot \Sigma_5 q + \tilde{U}_k(\Sigma, \Sigma^\dagger) \right\},$$

Baryon Number Fluctuations in 2+1 Flavor



Rui Wen, Chuang Huang, WF, in preparation

't Hooft determinant

$$\xi = \det(\Sigma) + \det(\Sigma^\dagger),$$

2+1 flavor PQM:

$$\Gamma_k = \int_x \left\{ \bar{q} [\gamma_\mu \partial_\mu - \gamma_0 (\mu + igA_0)] q + V_{\text{glue}}(L, \bar{L}) \right. \\ \left. + \text{tr}(\partial_\mu \Sigma \cdot \partial_\mu \Sigma^\dagger) + i\bar{q} h_k \cdot \Sigma_5 q + \tilde{U}_k(\Sigma, \Sigma^\dagger) \right\},$$

scalar and pseudoscalar mesons in the octet and singlet:

$$\Sigma = T_a (\sigma_a + i\pi_a), \quad a = 0, 1, \dots, 8$$

$$\Sigma_5 = T_a (\sigma_a + i\gamma_5 \pi_a),$$

the effective potential

$$\tilde{U}_k(\Sigma, \Sigma^\dagger) = U_k(\rho_1, \tilde{\rho}_2) - c_k \xi - j_L \sigma_L - j_S \sigma_S,$$

$$\rho_1 = \text{tr}(\Sigma \cdot \Sigma^\dagger),$$

$$\tilde{\rho}_2 = \text{tr} \left(\Sigma \cdot \Sigma^\dagger - \frac{1}{2} \rho_1 \right)^2,$$

also see talk by Fabian

Net Baryon Number Probability Distribution

Net Baryon Number Probability Distribution

The probability distribution:

$$P(N; T, V, \mu) = \frac{Z(T, V, N)}{\mathcal{Z}(T, V, \mu)} \exp\left(\frac{\mu N}{T}\right),$$

canonical partition function



grand canonical partition function



Net Baryon Number Probability Distribution

The probability distribution:

$$P(N; T, V, \mu) = \frac{Z(T, V, N)}{\mathcal{Z}(T, V, \mu)} \exp\left(\frac{\mu N}{T}\right),$$

canonical partition function

grand canonical partition function

$$Z(T, V, N) = \frac{1}{2\pi} \int_0^{2\pi} d\theta e^{-i\theta N} \mathcal{Z}(T, V, \mu = iT\theta),$$

Net Baryon Number Probability Distribution

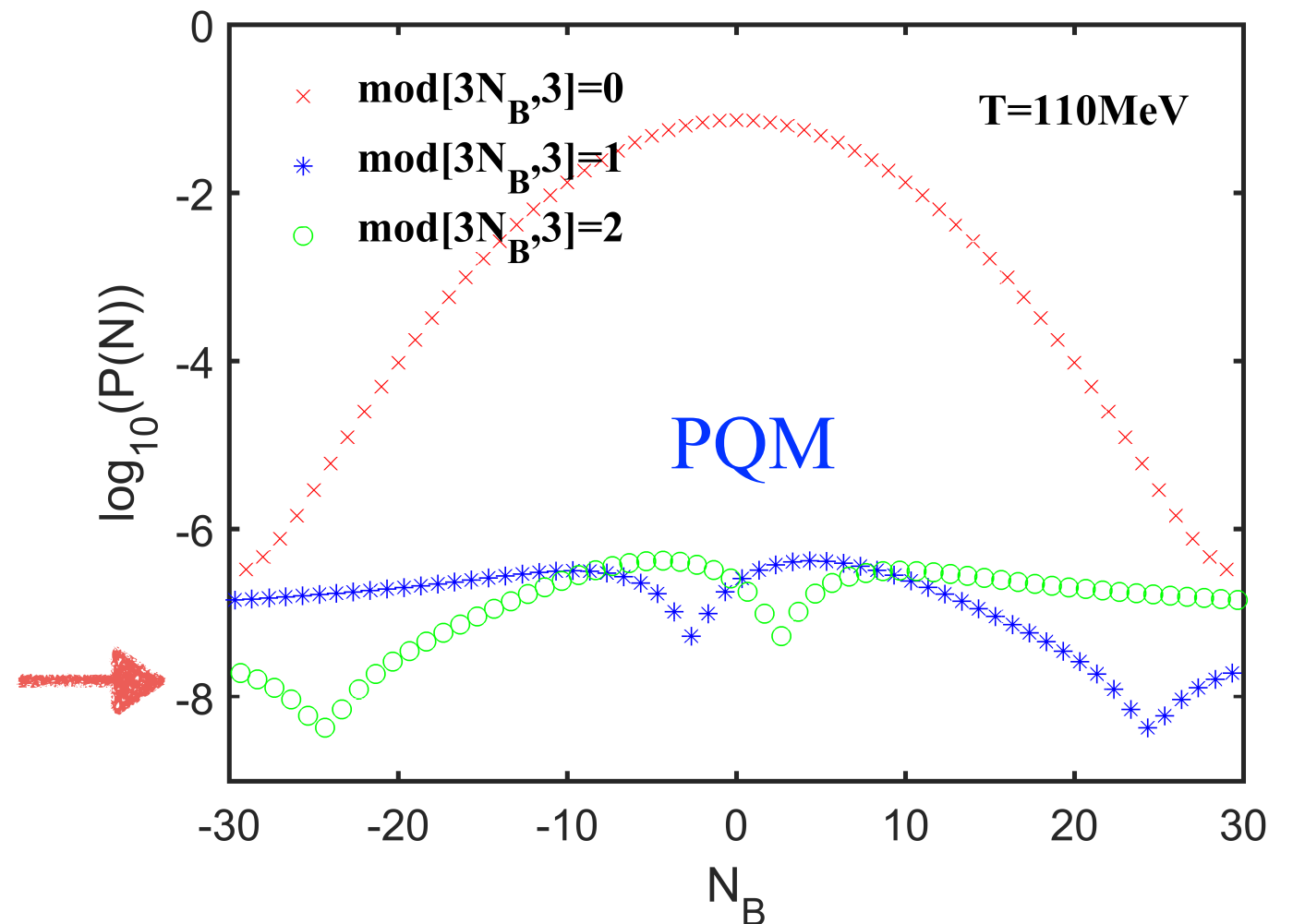
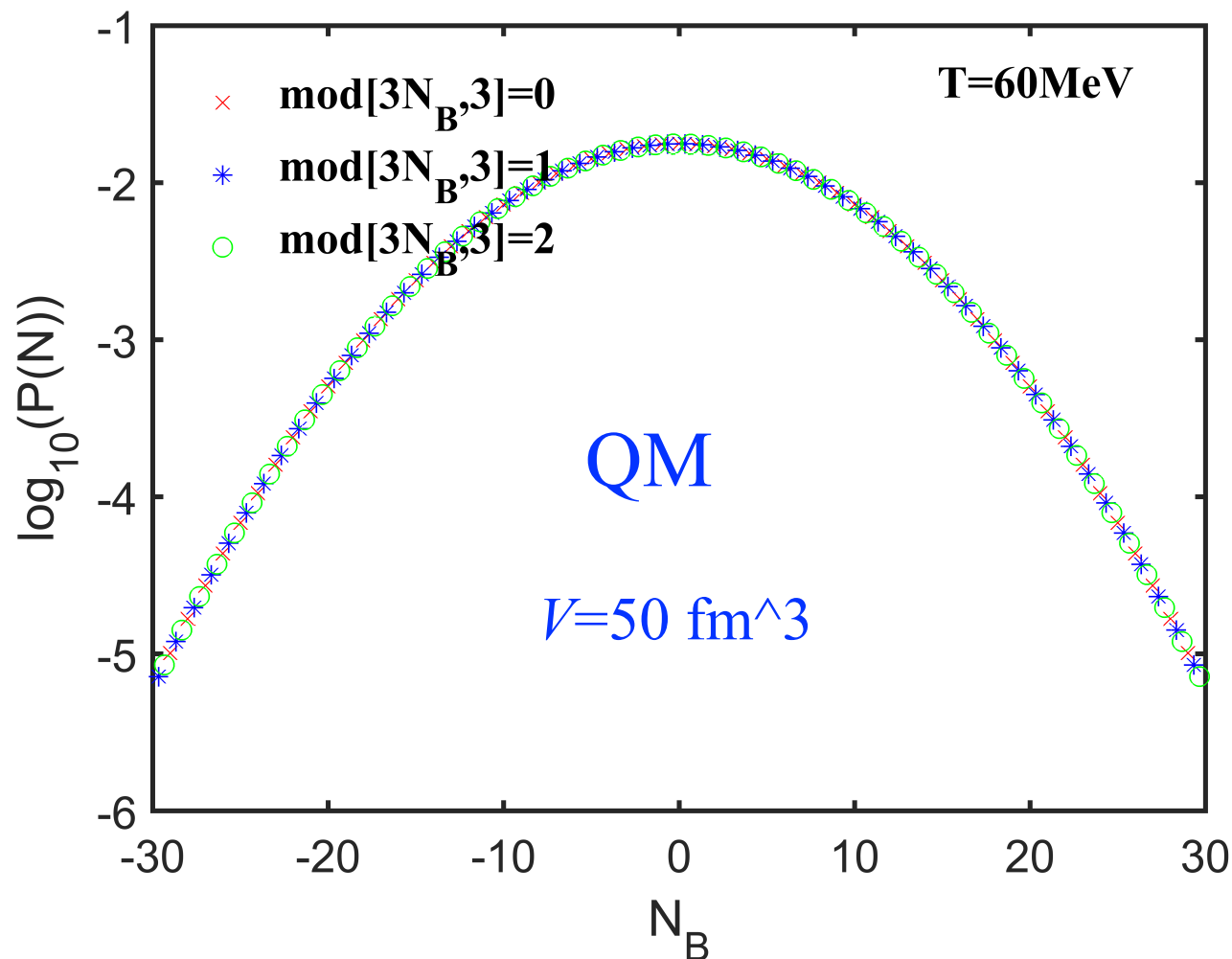
The probability distribution:

$$P(N; T, V, \mu) = \frac{Z(T, V, N)}{\mathcal{Z}(T, V, \mu)} \exp\left(\frac{\mu N}{T}\right),$$

canonical partition function

grand canonical partition function

$$Z(T, V, N) = \frac{1}{2\pi} \int_0^{2\pi} d\theta e^{-i\theta N} \mathcal{Z}(T, V, \mu = iT\theta),$$



Net Baryon Number Probability Distribution

Net Baryon Number Probability Distribution

Why do we need to calculate the probability distribution?

Net Baryon Number Probability Distribution

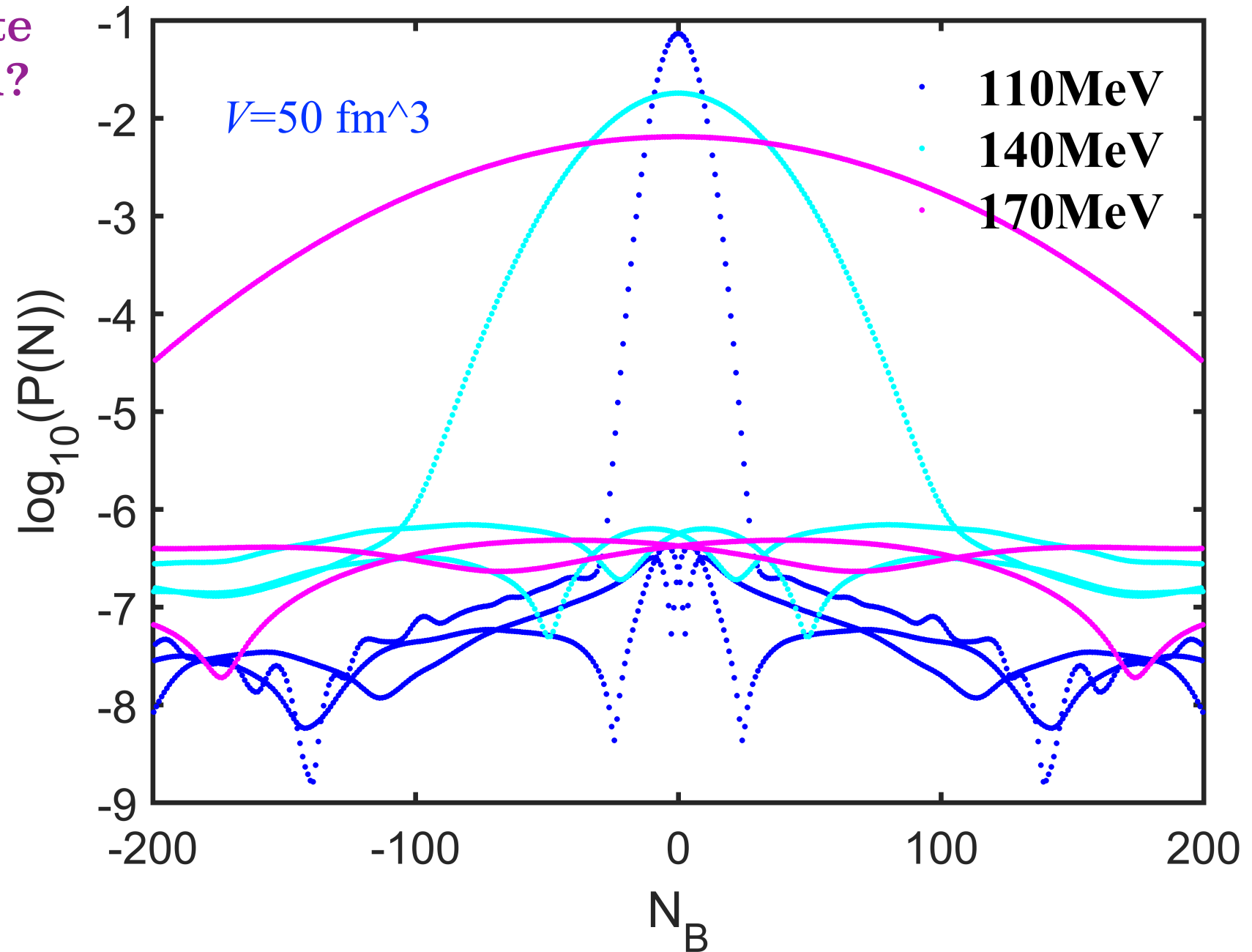
Why do we need to calculate the probability distribution?

- Sensitive to different dynamics, especially the glue dynamics.
- Input to transport simulations in heavy ion collisions
- Non-critical effects are easily involved, such as the detector acceptability cut, volume fluctuations etc.
- Related investigations are in progress.

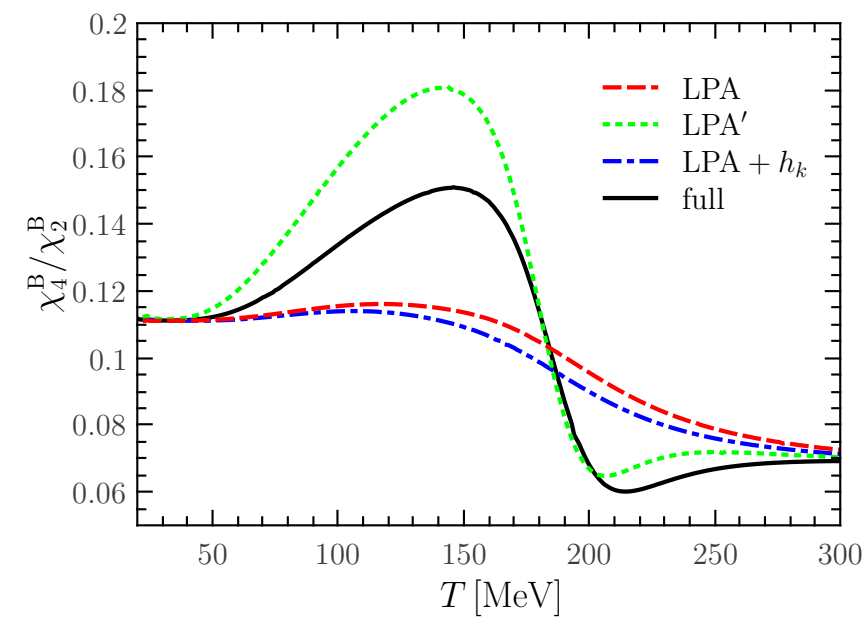
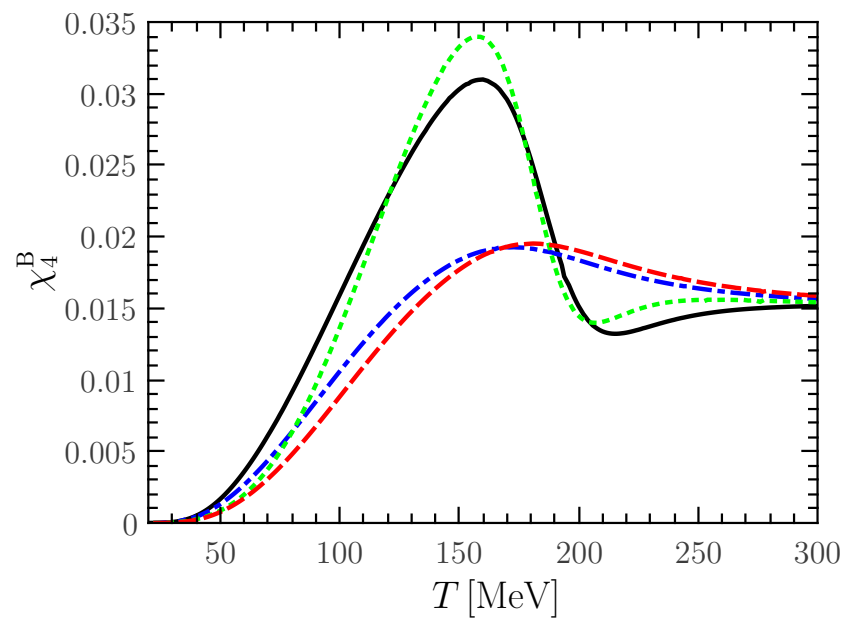
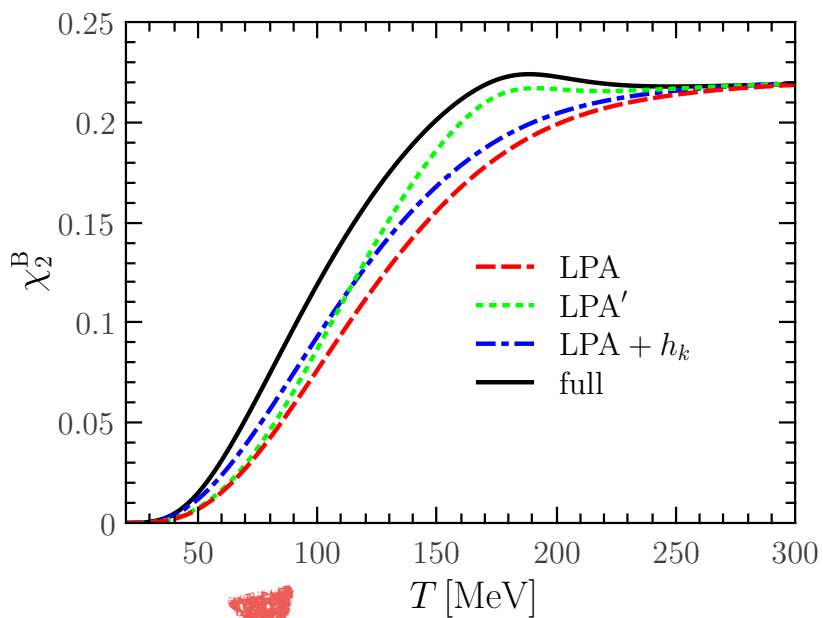
Net Baryon Number Probability Distribution

Why do we need to calculate the probability distribution?

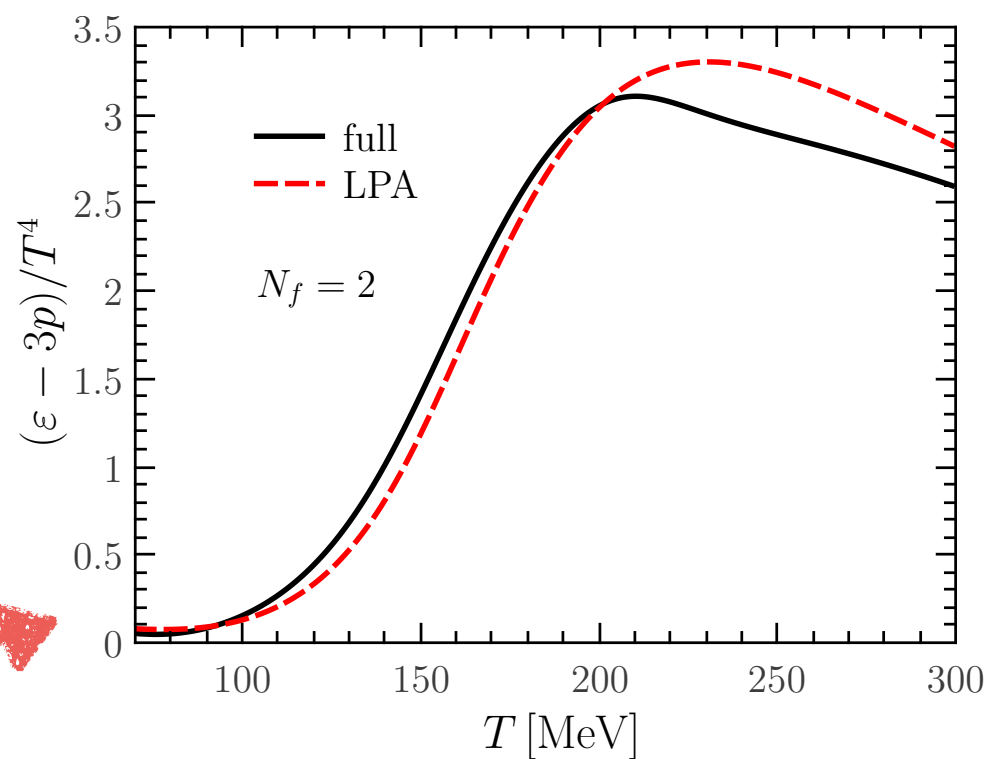
- Sensitive to different dynamics, especially the glue dynamics.
- Input to transport simulations in heavy ion collisions
- Non-critical effects are easily involved, such as the detector acceptability cut, volume fluctuations etc.
- Related investigations are in progress.



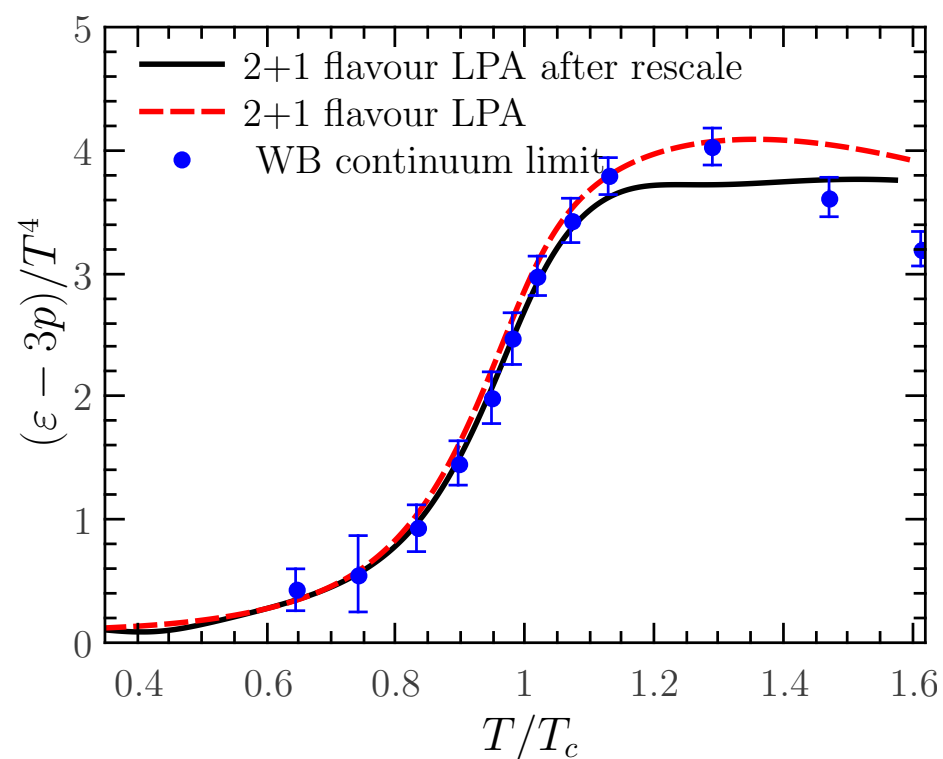
Quantum Fluctuations beyond LPA



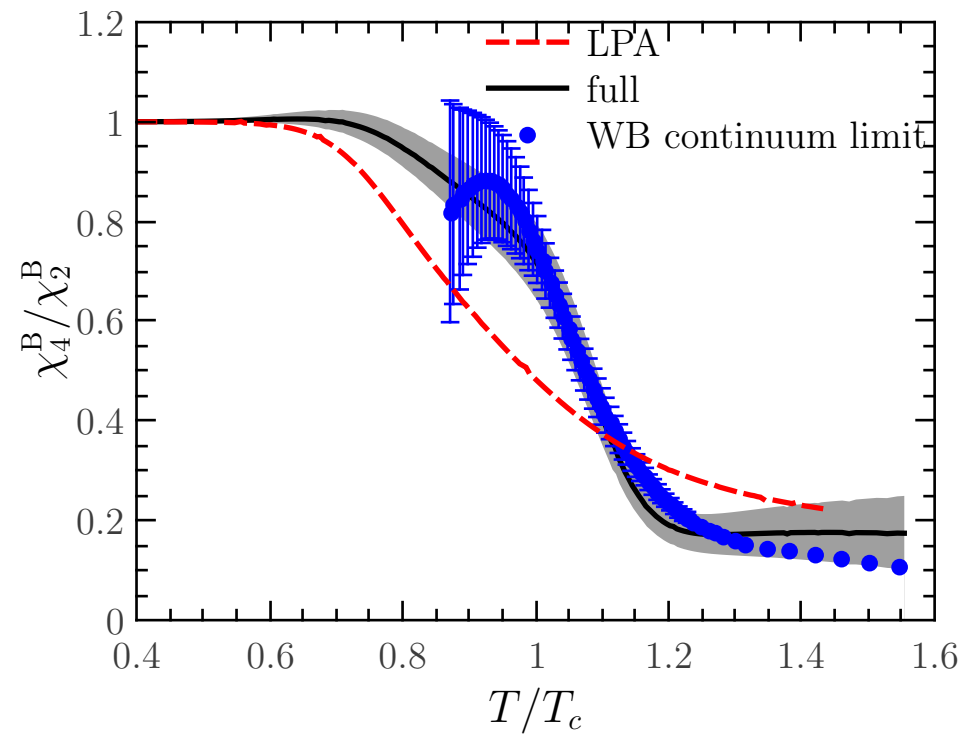
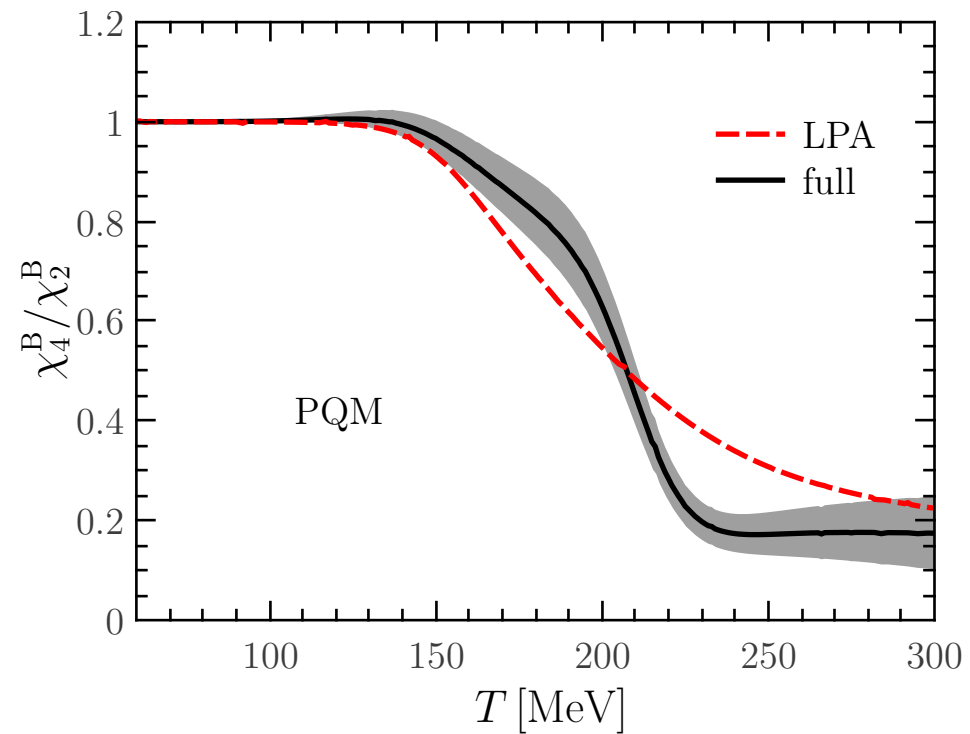
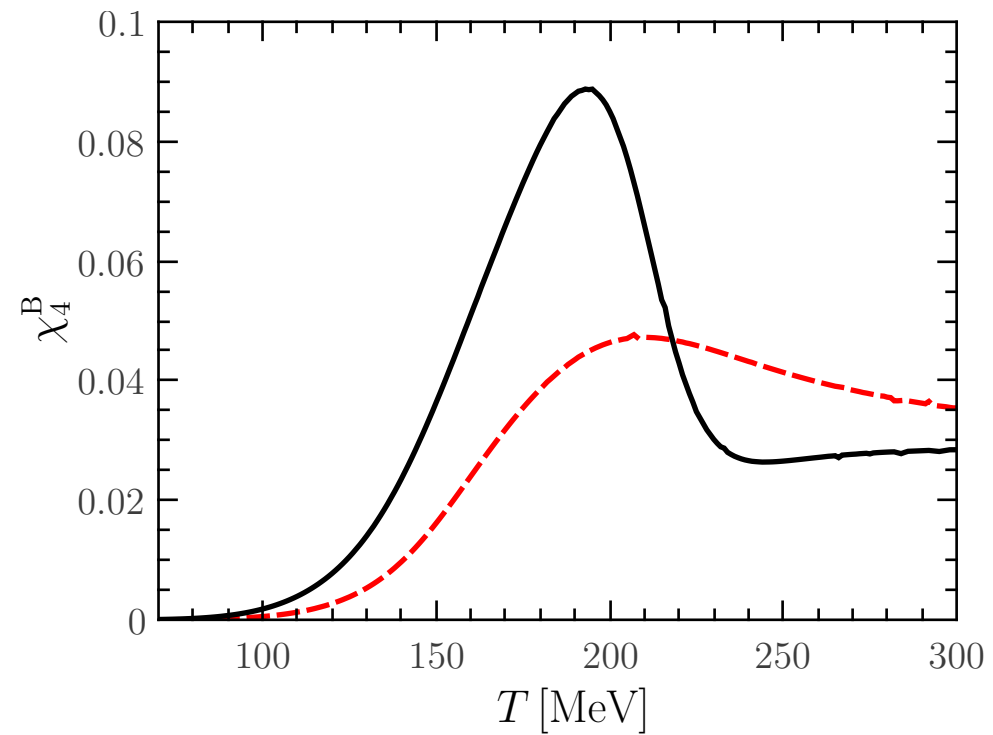
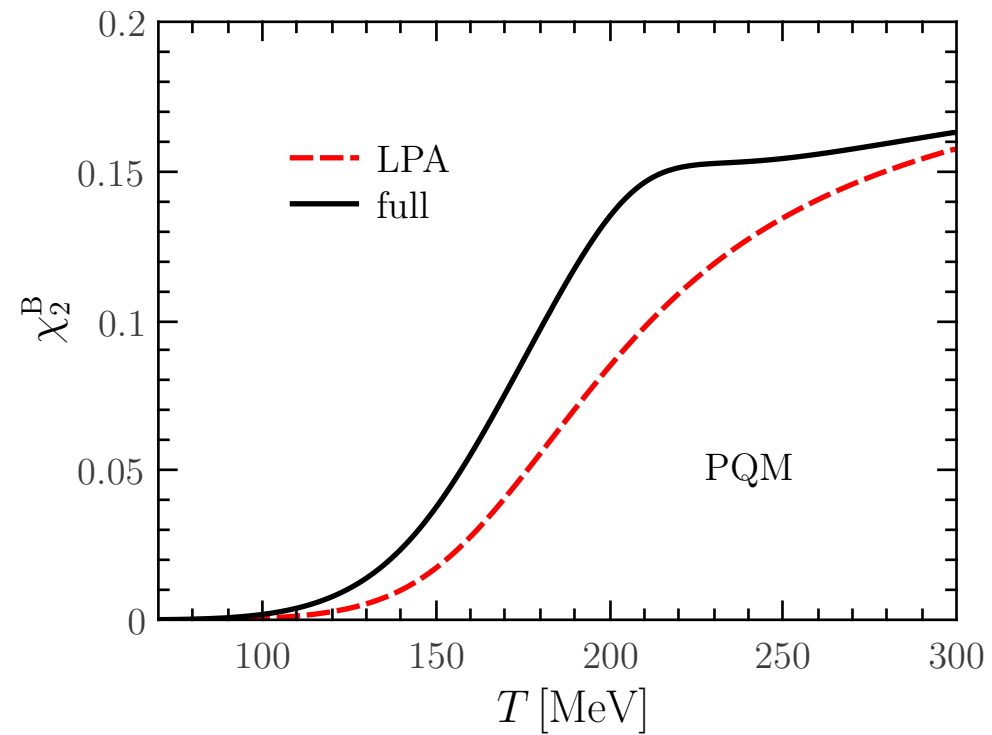
QM



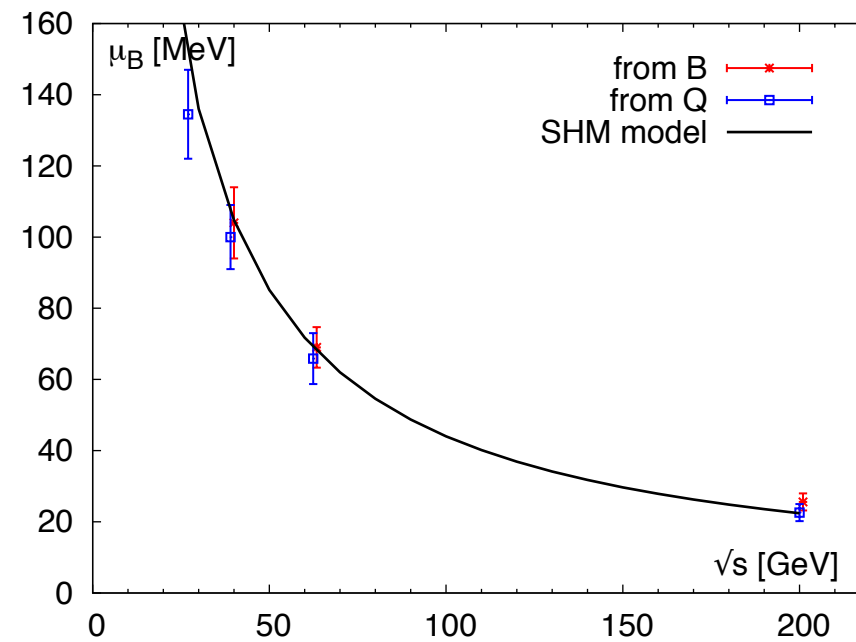
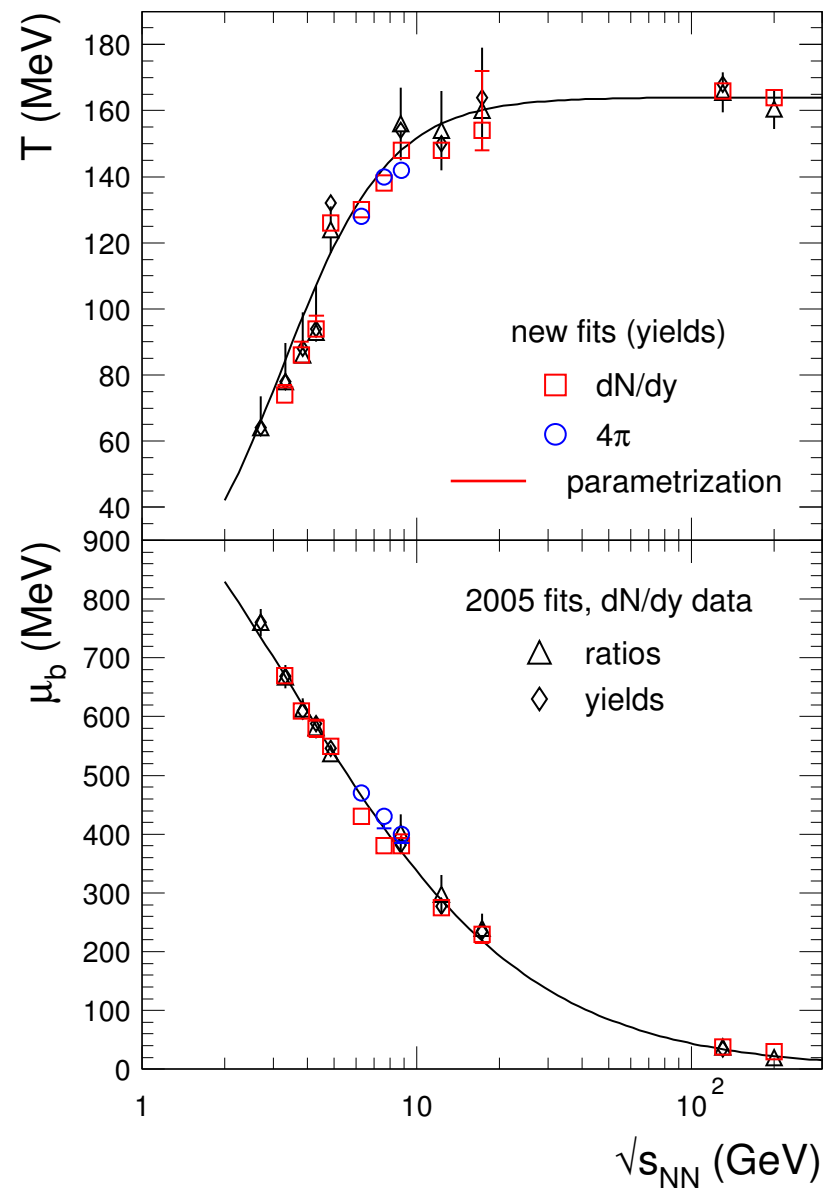
PQM



Baryon number fluctuations beyond LPA



Freeze-out line



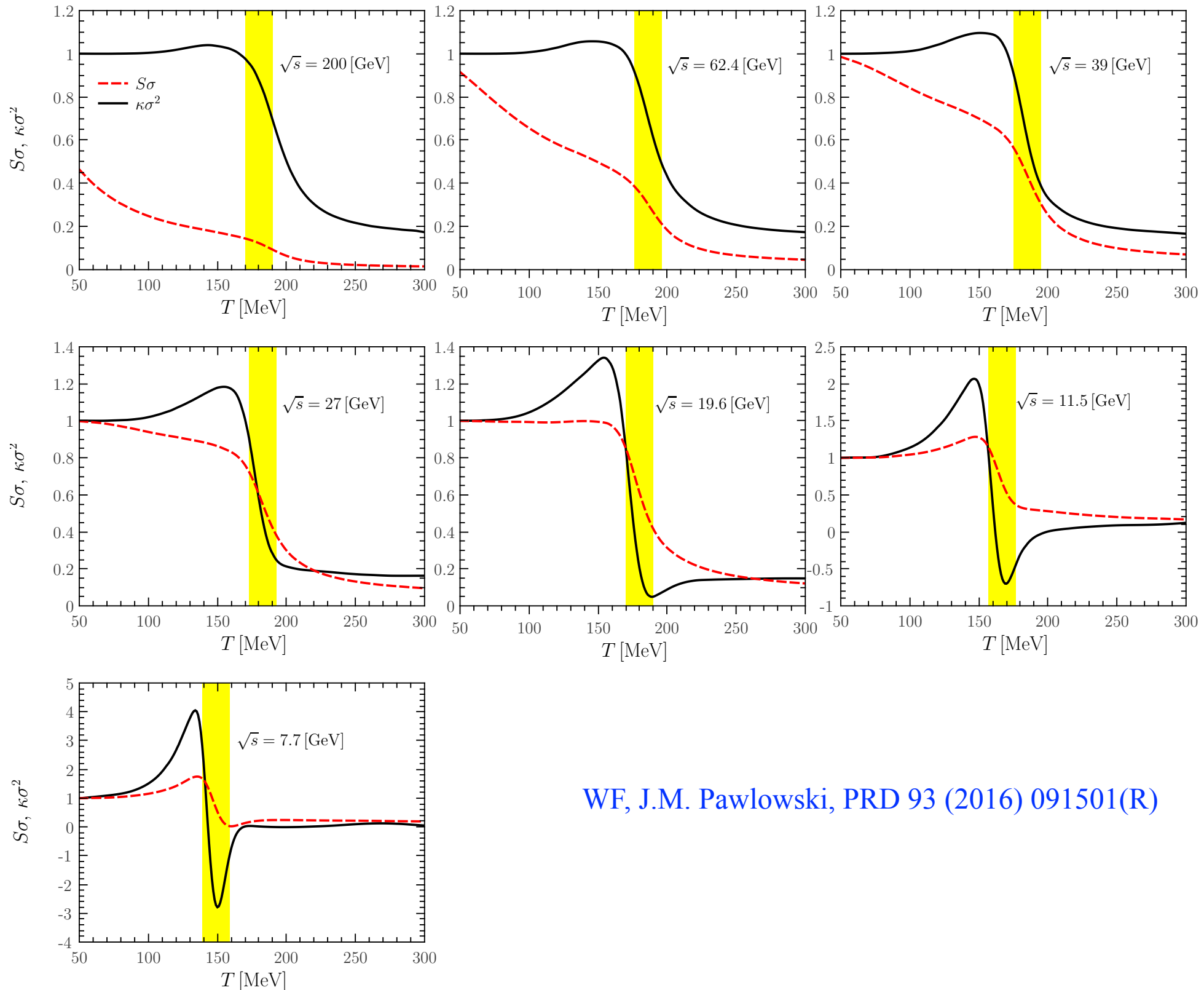
Freeze-out chemical potential obtained from lattice simulations

S. Borsanyi *et al.*, Phys.Rev.Lett. 113 (2014) 052301

Freeze-out temperature and chemical potential obtained from the Statistical Hadronization Model

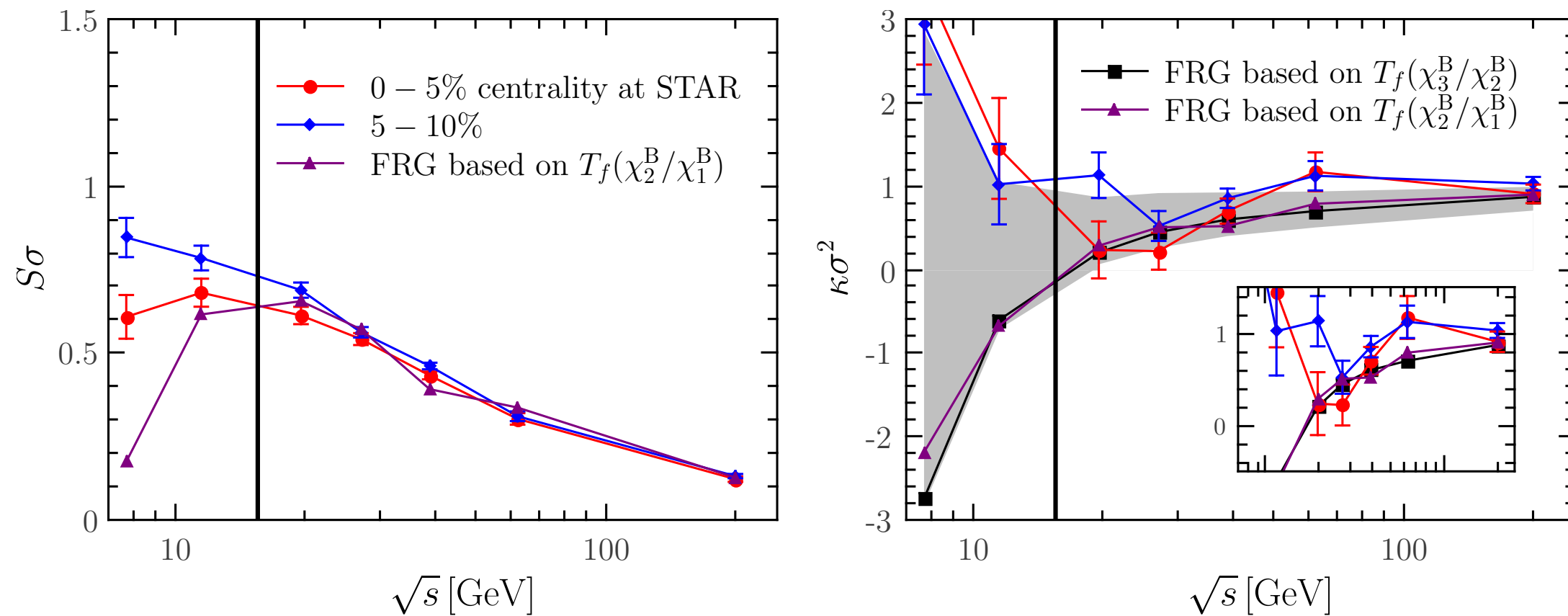
A. Andronic, P. Braun-Munzinger, J. Stachel, Phys.Lett. B673 (2009) 142

Correlating the skewness and kurtosis of baryon number distributions



WF, J.M. Pawłowski, PRD 93 (2016) 091501(R)

Comparison with experimental measurements



WF, J.M. Pawlowski, PRD 93 (2016) 091501(R)

Silver Blaze Property and the Frequency Dependence

Frequency-dependent quark anomalous dimension:

$$\eta_{q,k}(p) = \frac{1}{Z_{q,k}(p)} \frac{1}{4N_c N_f} \frac{\partial^2}{\partial |\vec{p}|^2} \text{Tr} \left(i\vec{\gamma} \cdot \vec{p} \partial_t \tilde{\Gamma}_{q\bar{q},k}^{(2)}(p) \right)$$

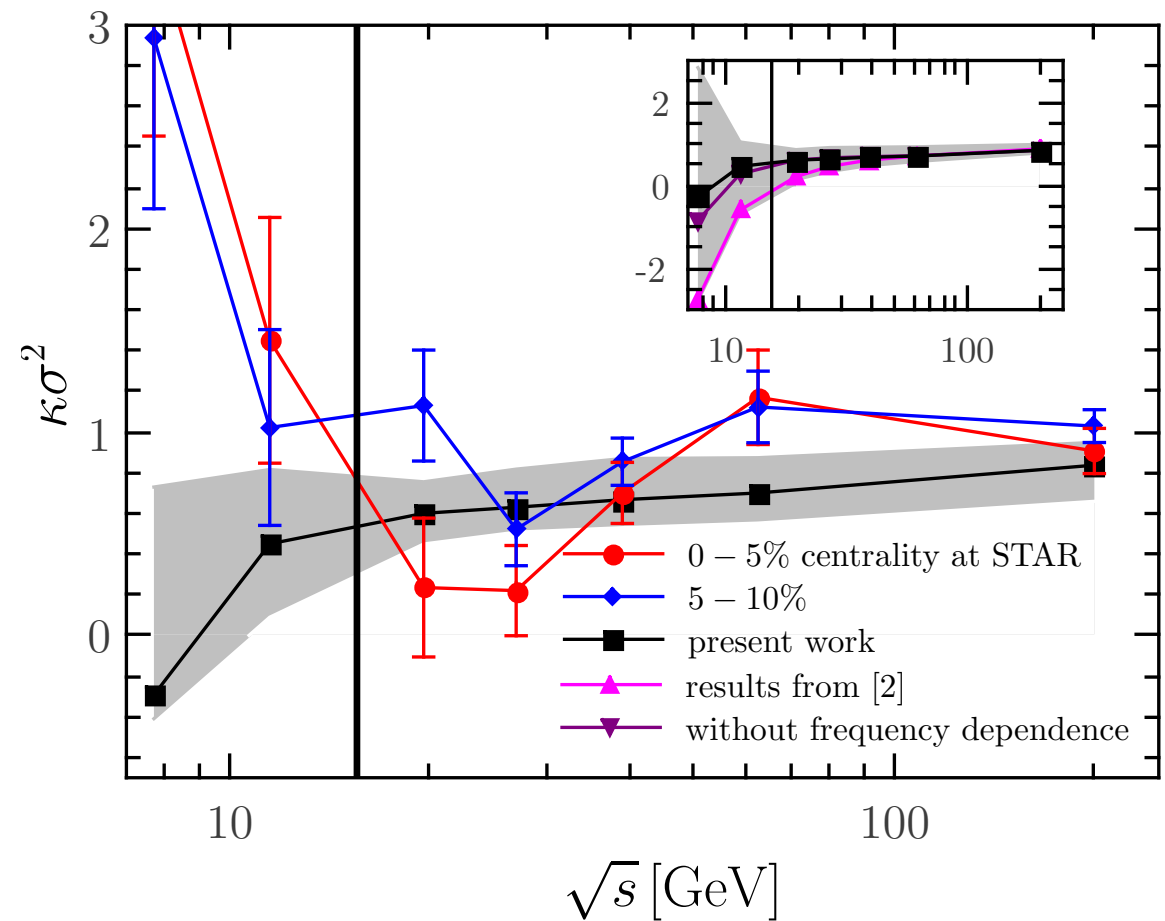
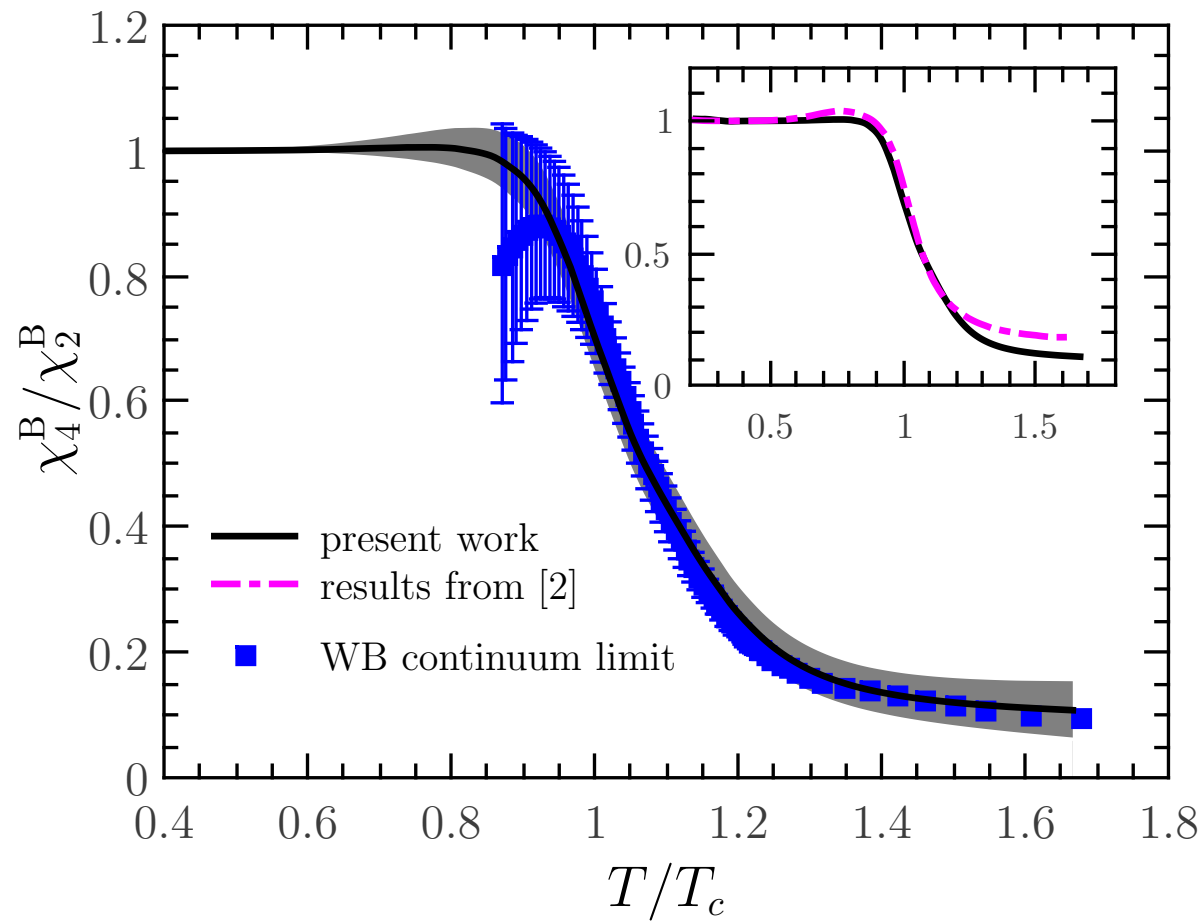
Insert this into the flow of effective potential, and perform the two-loop summation

$$\partial_t V_k^q = - \int_q \text{circle with } \otimes \text{ and } q \text{ arrows} \approx - \iint_{p,q} \text{circle with } \otimes \text{ and } p, q \text{ arrows}$$

One obtains

$$\begin{aligned} \partial_t V_k(\rho) = & \frac{k^4}{360\pi^2} \left\{ 12(5 - \eta_{\phi,k}) \left[(N_f^2 - 1) \mathcal{B}_{(1)}(\bar{m}_{\pi,k}^2) \right. \right. \\ & + \left. \mathcal{B}_{(1)}(\bar{m}_{\sigma,k}^2) \right] - 5N_c \left(48N_f \mathcal{F}_{(1)}(\bar{m}_{F,k}^2) \right. \\ & + \frac{1}{2\pi^2} (-4 + \eta_{\phi,k}) \bar{h}_k^2 \left[\mathcal{FFB}_{(1,1,2)}(\bar{m}_{F,k}^2, \bar{m}_{\sigma,k}^2) \right. \\ & \left. \left. + (N_f^2 - 1) \mathcal{FFB}_{(1,1,2)}(\bar{m}_{F,k}^2, \bar{m}_{\pi,k}^2) \right] \right) \left. \right\}, \end{aligned}$$

Two-loop Results



$$\partial_t V_k^q = - \int_q \text{[Diagram 1]} \approx - \iint_{p,q} \text{[Diagram 2]}$$

Diagram 1: A circular loop with a cross in a circle at the top and an arrow labeled q at the bottom.

 Diagram 2: A circular loop with a cross in a circle at the top, an arrow labeled p at the top, an arrow labeled $p+q$ at the top, and an arrow labeled q at the bottom.

From effective models to QCD

Summary on effective model including mesonic fluctuations

- Quantitative agreement with lattice results below $\sim 1.2 T_c$
- No bump on the baryon number kurtosis
- Discrepancy observed at large temperature or density because of the UV cutoff effect
- UV cutoff should be pushed up higher, and glue quantum fluctuations should be included

From effective models to QCD

Summary on effective model including mesonic fluctuations

$$\partial_t \Gamma_k = \frac{1}{2} \left(\text{diagram 1} - \text{diagram 2} - \text{diagram 3} + \frac{1}{2} \text{diagram 4} \right)$$

- Quantitative agreement with lattice results below $\sim 1.2 T_c$
- No bump on the baryon number kurtosis
- Discrepancy observed at large temperature or density because of the UV cutoff effect
- UV cutoff should be pushed up higher, and glue quantum fluctuations should be included

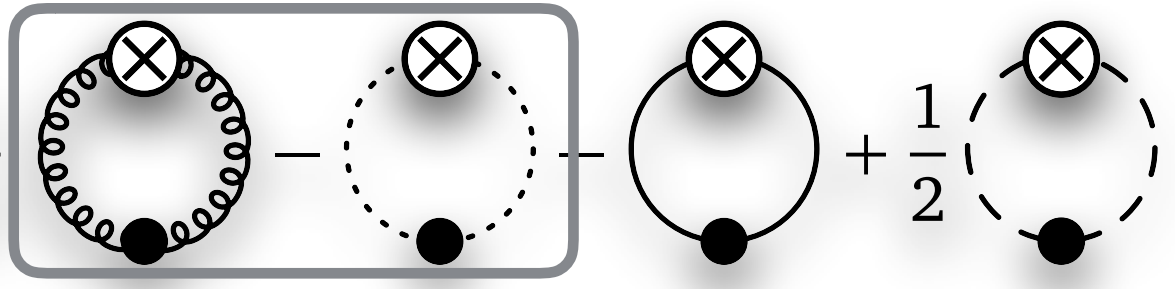
From effective models to QCD

Summary on effective model including mesonic fluctuations

- Quantitative agreement with lattice results below $\sim 1.2 T_c$
- No bump on the baryon number kurtosis
- Discrepancy observed at large temperature or density because of the UV cutoff effect
- UV cutoff should be pushed up higher, and glue quantum fluctuations should be included

$$\partial_t \Gamma_k = \frac{1}{2} \left[\text{Diagram 1} - \text{Diagram 2} \right] - \text{Diagram 3} + \frac{1}{2} \text{Diagram 4}$$

Come back!



The diagram shows the derivative of the effective action $\partial_t \Gamma_k$ as a sum of four terms. The first two terms are enclosed in a box and are subtracted from each other. The first term in the box is a loop with a wavy line and a cross in a circle. The second term in the box is a loop with a dashed line and a cross in a circle. The third term is a loop with a solid line and a cross in a circle. The fourth term is a loop with a dashed line and a cross in a circle, multiplied by $\frac{1}{2}$. A red arrow points from the text 'Come back!' to the first diagram in the box.

From effective models to QCD

Summary on effective model including mesonic fluctuations

- Quantitative agreement with lattice results below $\sim 1.2 T_c$
- No bump on the baryon number kurtosis
- Discrepancy observed at large temperature or density because of the UV cutoff effect
- UV cutoff should be pushed up higher, and glue quantum fluctuations should be included

$$\partial_t \Gamma_k = \frac{1}{2} \left[\text{diagram 1} - \text{diagram 2} \right] - \text{diagram 3} + \frac{1}{2} \text{diagram 4}$$

Come back!

Effective model:

$$\Gamma_k = \int_x \left\{ Z_{q,k} \bar{q} (\gamma_\mu \partial_\mu - \gamma_0 \mu) q + \frac{1}{2} Z_{\phi,k} (\partial_\mu \phi)^2 + h_k \bar{q} \left(T^0 \sigma + i \gamma_5 \vec{T} \cdot \vec{\pi} \right) q + V_k(\rho) - c\sigma \right\} + \dots$$

From effective models to QCD

Summary on effective model including mesonic fluctuations

- Quantitative agreement with lattice results below $\sim 1.2 T_c$
- No bump on the baryon number kurtosis
- Discrepancy observed at large temperature or density because of the UV cutoff effect
- UV cutoff should be pushed up higher, and glue quantum fluctuations should be included

$$\partial_t \Gamma_k = \frac{1}{2} \left[\text{diagram 1} - \text{diagram 2} \right] - \text{diagram 3} + \frac{1}{2} \text{diagram 4}$$

Come back!

Effective model:

$$\Gamma_k = \int_x \left\{ Z_{q,k} \bar{q} (\gamma_\mu \partial_\mu - \gamma_0 \mu) q + \frac{1}{2} Z_{\phi,k} (\partial_\mu \phi)^2 + h_k \bar{q} \left(T^0 \sigma + i \gamma_5 \vec{T} \cdot \vec{\pi} \right) q + V_k(\rho) - c\sigma \right\} + \dots$$

Rebosonized QCD:

$$\Gamma_k = \int_x \left\{ \frac{1}{4} F_{\mu\nu}^a F_{\mu\nu}^a + Z_{c,k} (\partial_\mu \bar{c}^a) D_\mu^{ab} c^b + \frac{1}{2\xi} (\partial_\mu A_\mu^a)^2 + Z_{q,k} \bar{q} (\gamma_\mu D_\mu) q - \lambda_{q,k} [(\bar{q} T^0 q)^2 - (\bar{q} \gamma_5 \vec{T} q)^2] + h_k [\bar{q} (i \gamma_5 \vec{T} \vec{\pi} + T^0 \sigma) q] + \frac{1}{2} Z_{\phi,k} (\partial_\mu \phi)^2 + V_k(\rho) - c\sigma \right\} + \Delta \Gamma_{\text{glue}}$$

2 flavor

Flow Equations

Wetterich equation:

$$\begin{aligned}\partial_t \Gamma_k[\Phi] &= \frac{1}{2} \text{STr} \left\{ \partial_t R_k (\Gamma_k^{(2)}[\Phi] + R_k)^{-1} \right\} \\ &= \frac{1}{2} \text{STr} \left\{ \tilde{\partial}_t \ln (\Gamma_k^{(2)}[\Phi] + R_k) \right\}\end{aligned}$$

with $t = \ln(k/\Lambda)$ and

$$(\Gamma_k^{(2)}[\Phi])_{ij} := \frac{\overrightarrow{\delta}}{\delta \Phi_i} \Gamma_k[\Phi] \frac{\overleftarrow{\delta}}{\delta \Phi_j} \quad \Gamma_k^{(2)} + R_k = \mathcal{P} + \mathcal{F}$$

Vertex expansion:

$$\begin{aligned}\partial_t \Gamma_k &= \frac{1}{2} \text{STr} \{ \tilde{\partial}_t \ln(\mathcal{P} + \mathcal{F}) \} = \frac{1}{2} \text{STr} \tilde{\partial}_t \ln \mathcal{P} \\ &+ \frac{1}{2} \text{STr} \tilde{\partial}_t \left(\frac{1}{\mathcal{P}} \mathcal{F} \right) - \frac{1}{4} \text{STr} \tilde{\partial}_t \left(\frac{1}{\mathcal{P}} \mathcal{F} \right)^2 + \dots\end{aligned}$$

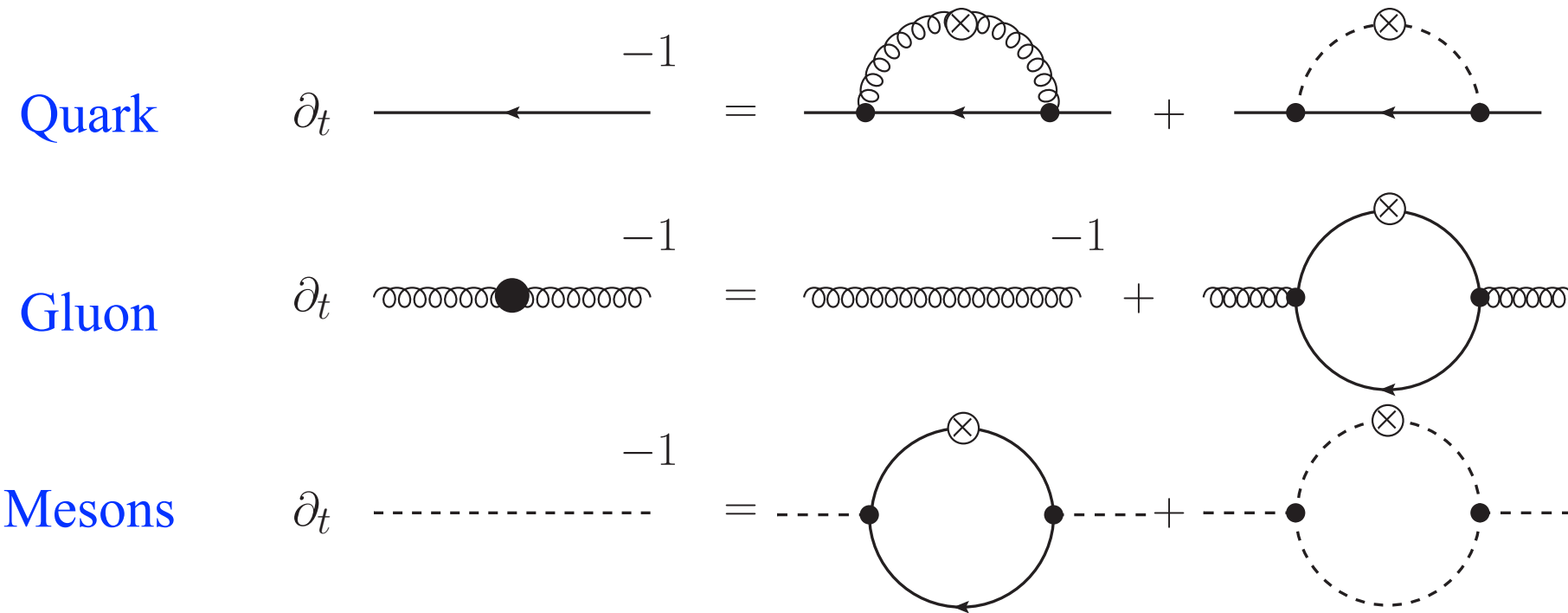
3d optimized regulator:

$$R_{\text{F},k}(q) = Z_{q,k} i \vec{q} \cdot \vec{\gamma} r_{\text{F}}\left(\frac{\vec{q}^2}{k^2}\right), \quad \text{with} \quad r_{\text{F}}(x) = \left(\frac{1}{\sqrt{x}} - 1\right) \Theta(1-x)$$

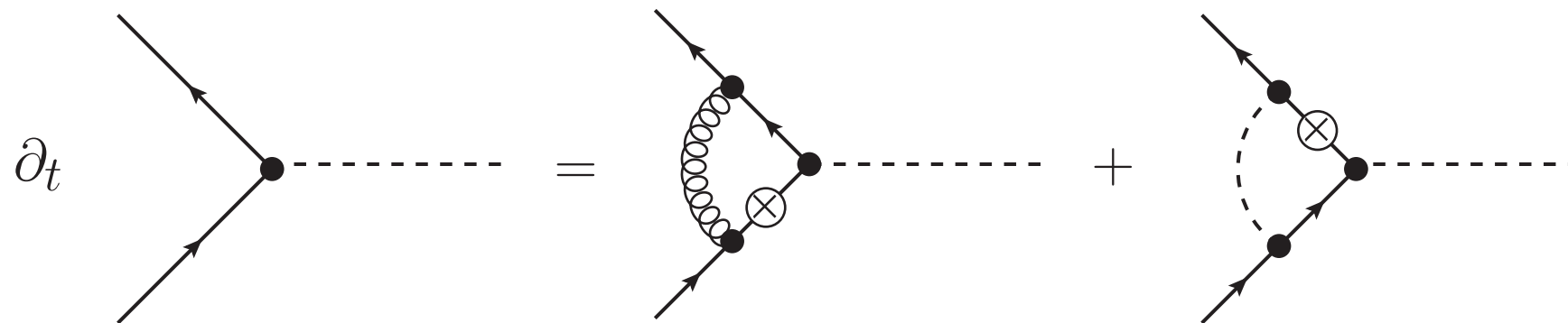
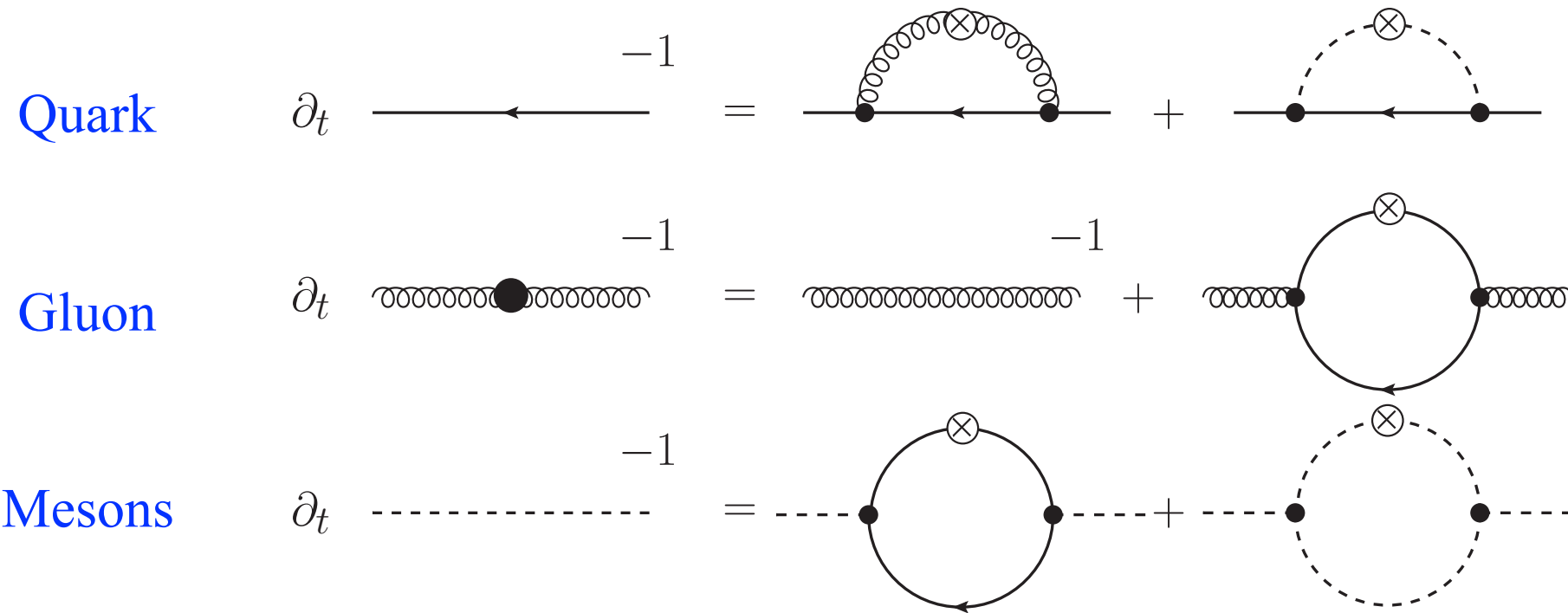
$$R_{\text{B},k}(q) = Z_{\phi,k} \vec{q}^2 r_{\text{B}}\left(\frac{\vec{q}^2}{k^2}\right), \quad \text{with} \quad r_{\text{B}}(x) = \left(\frac{1}{x} - 1\right) \Theta(1-x)$$

Feynman Diagrams

Feynman Diagrams

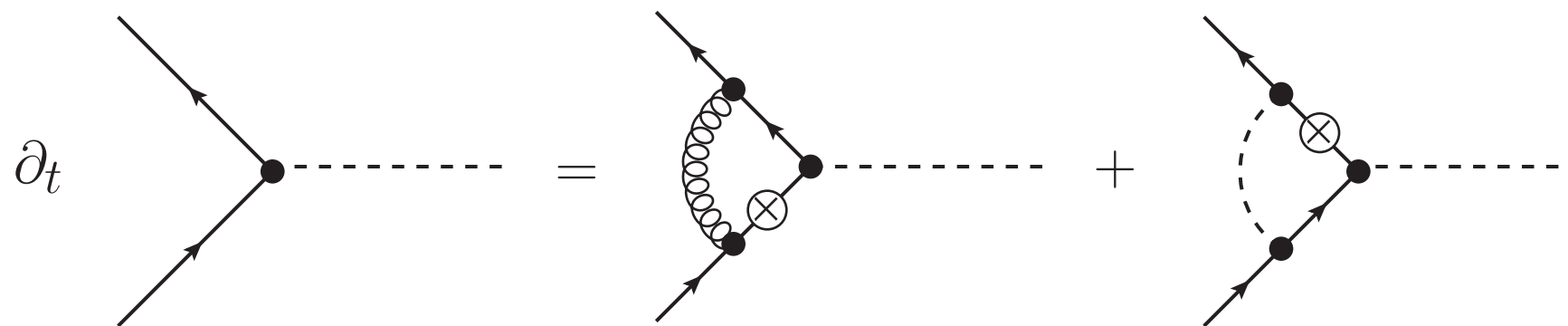


Feynman Diagrams



Yukawa coupling

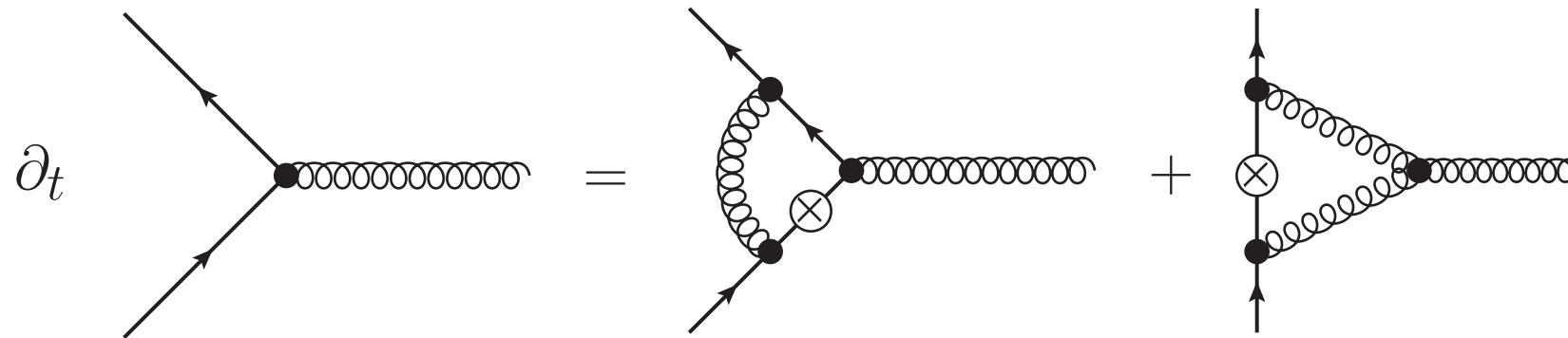
Feynman Diagrams



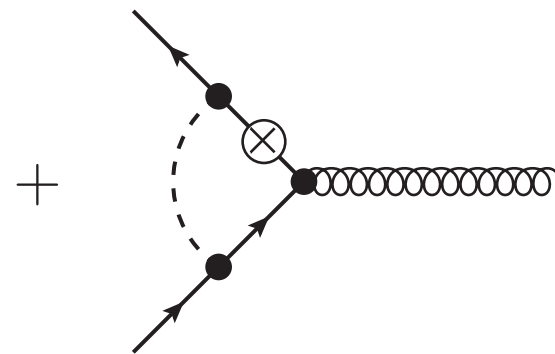
Yukawa coupling

Feynman Diagrams

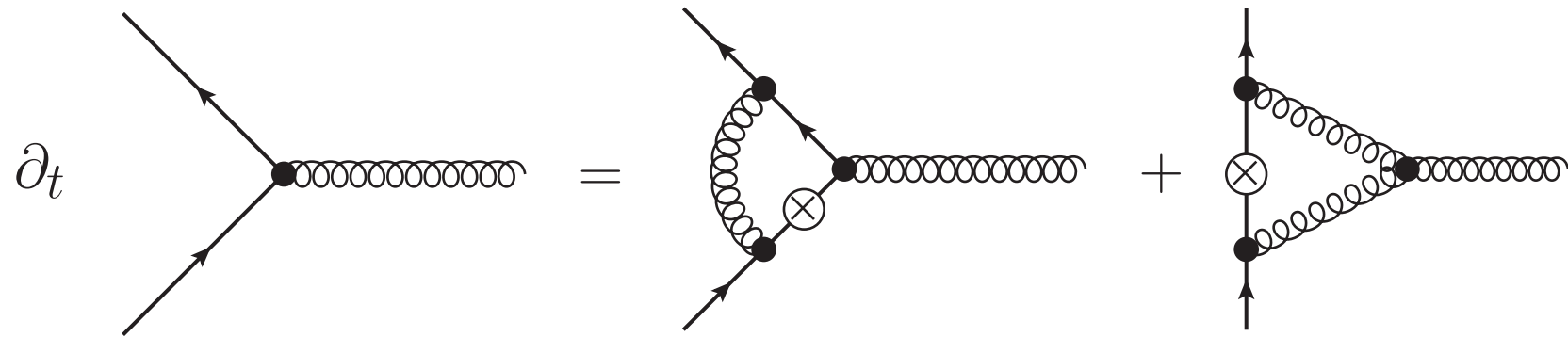
Feynman Diagrams



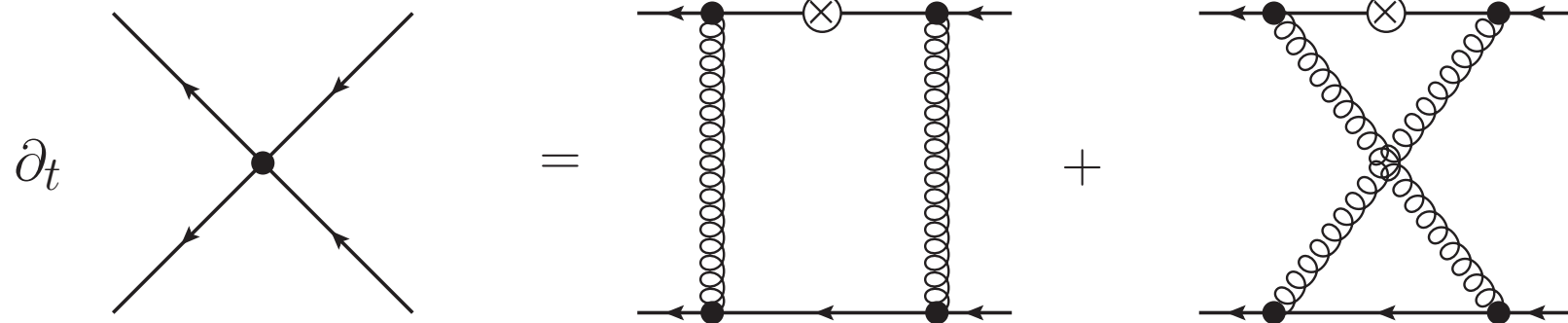
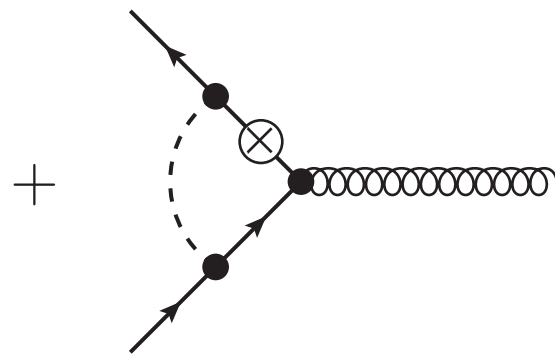
Quark gluon vertex



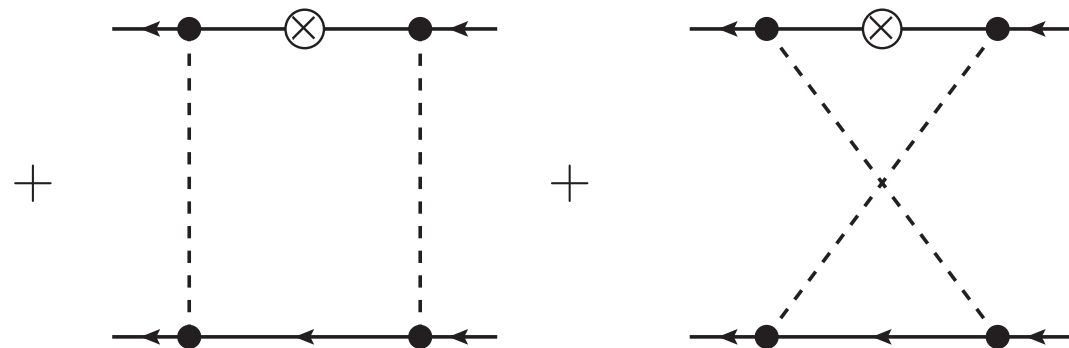
Feynman Diagrams



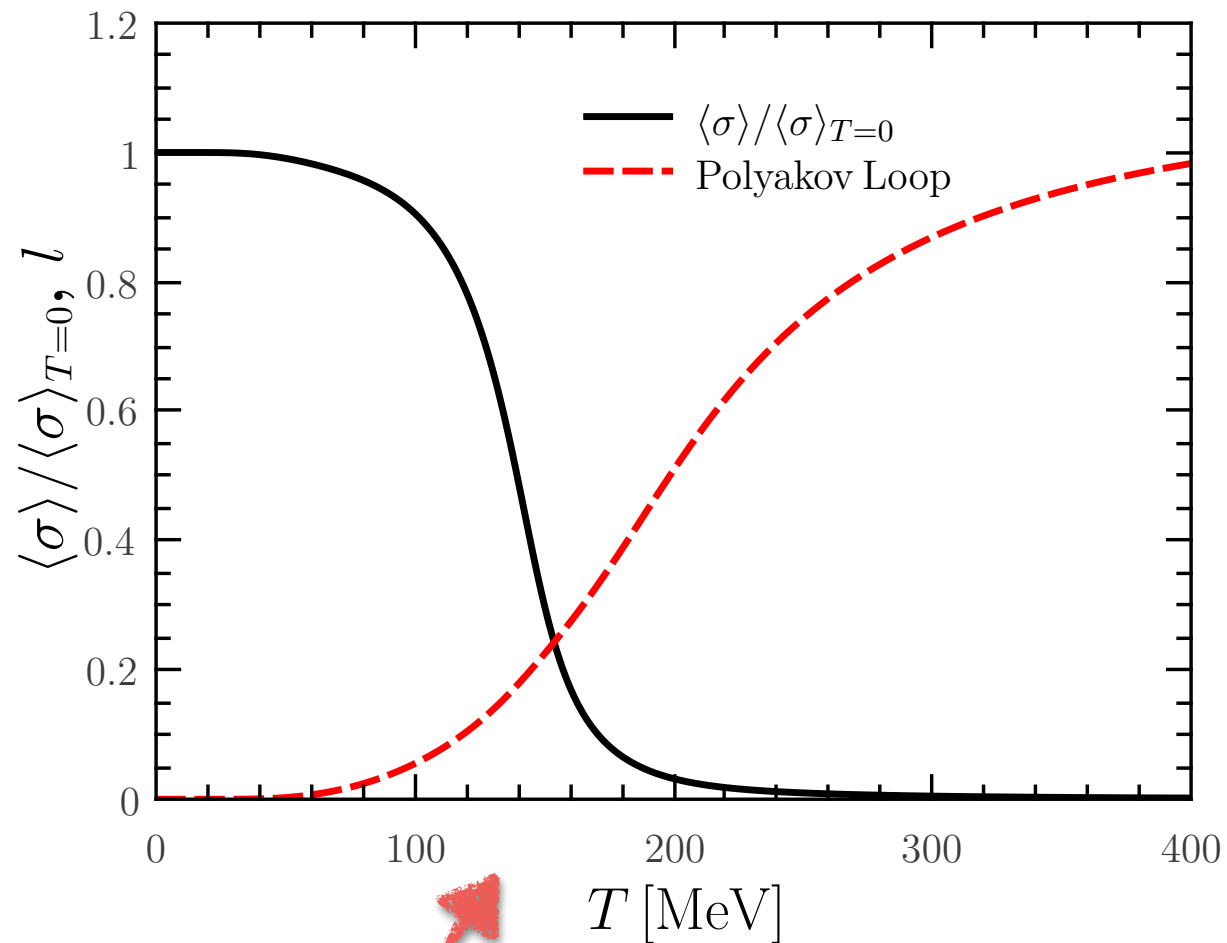
Quark gluon vertex



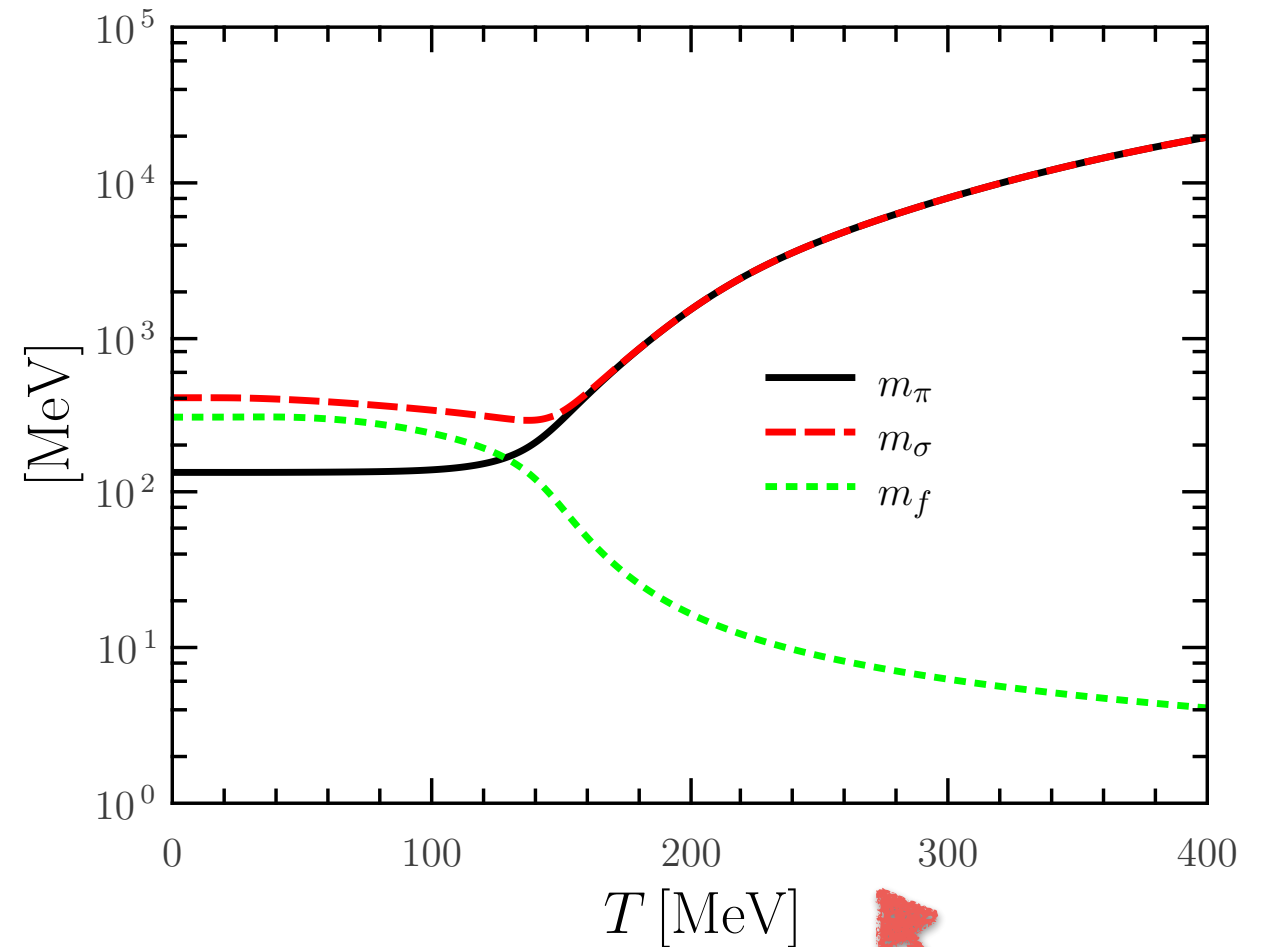
Four-fermion coupling



QCD Phase Transition with T

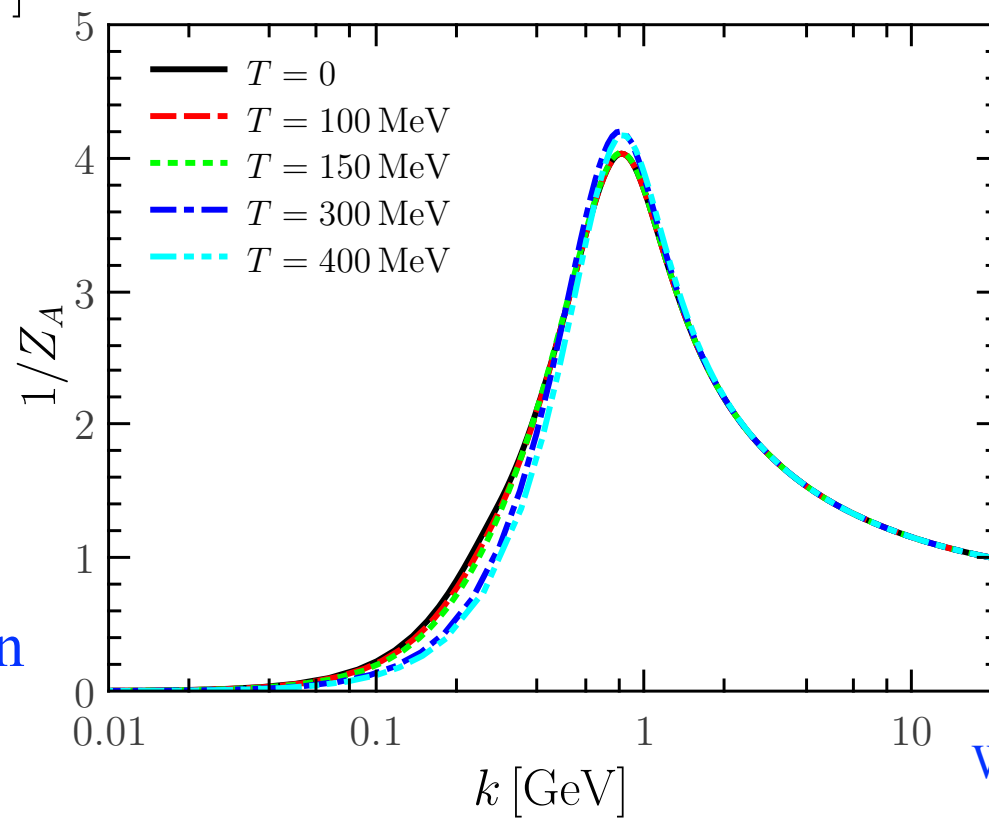
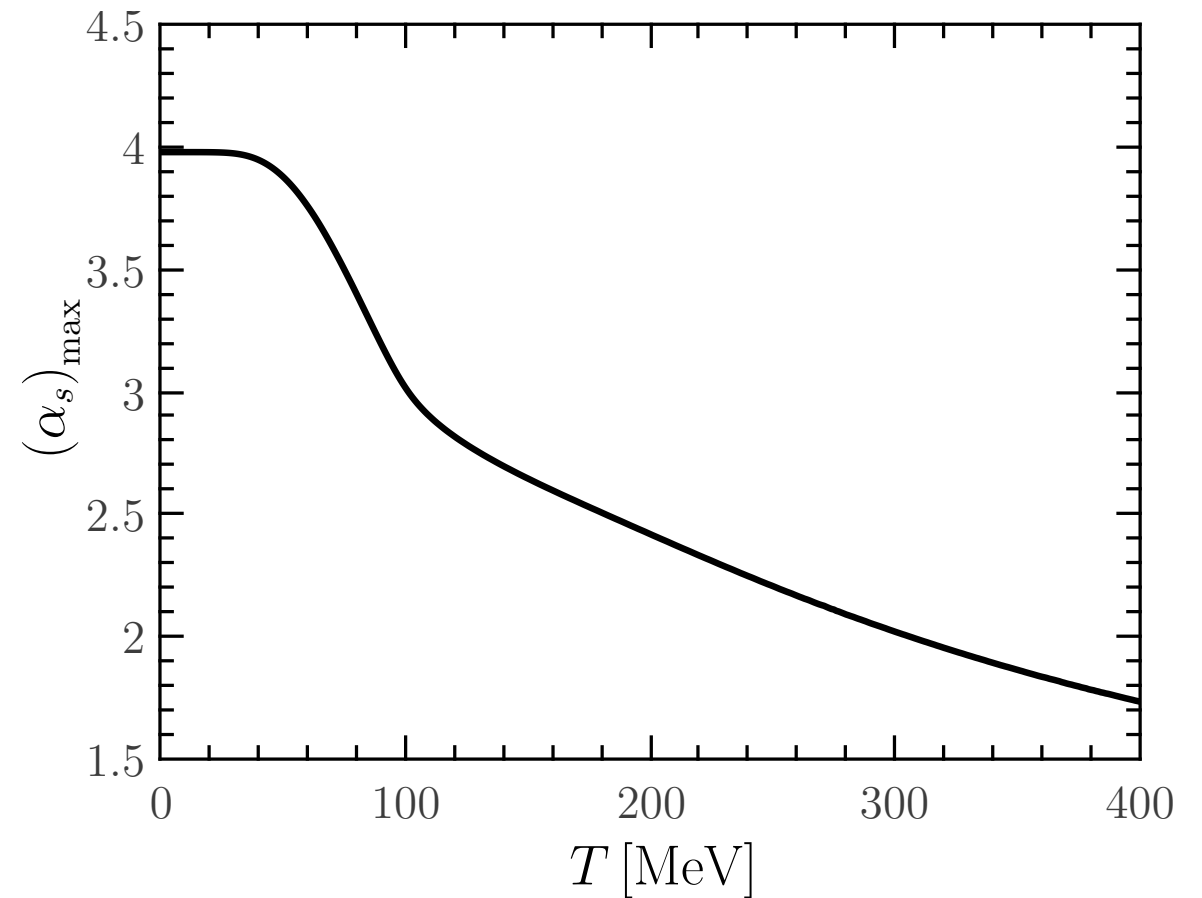
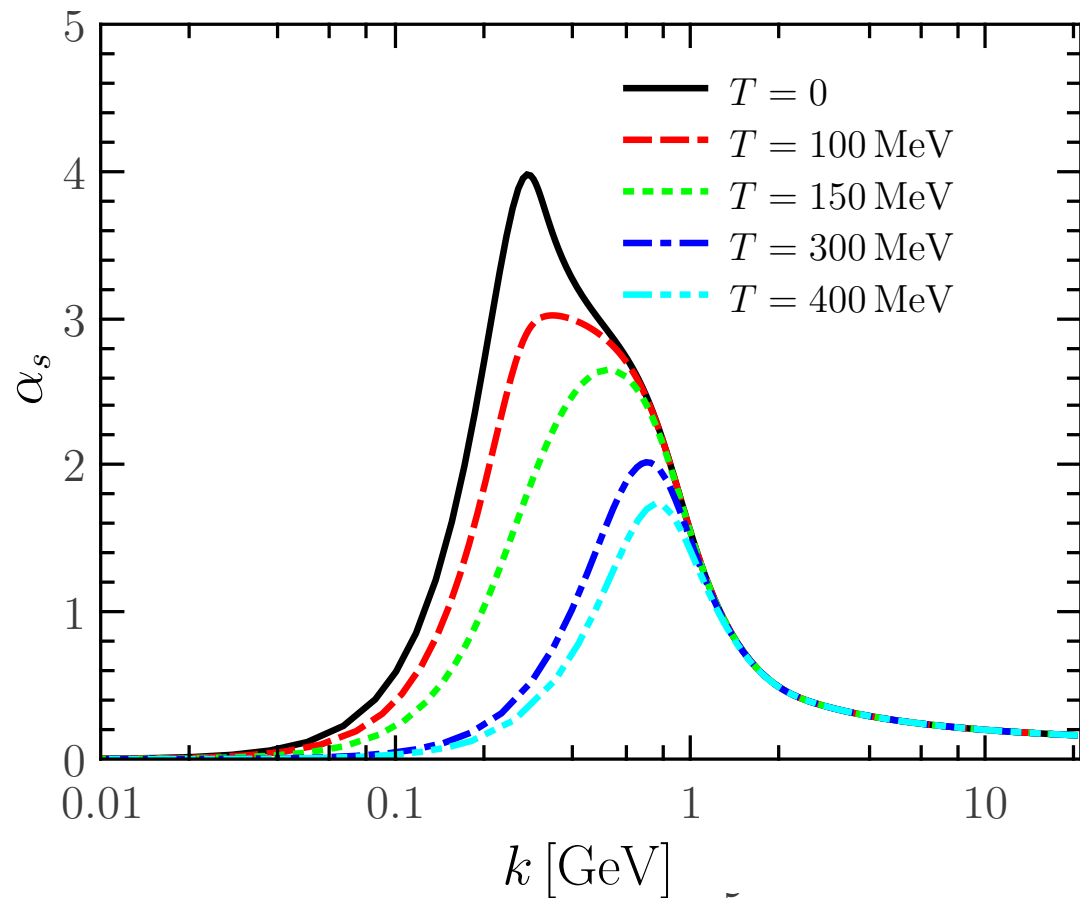


Order parameter



Meson and quark mass

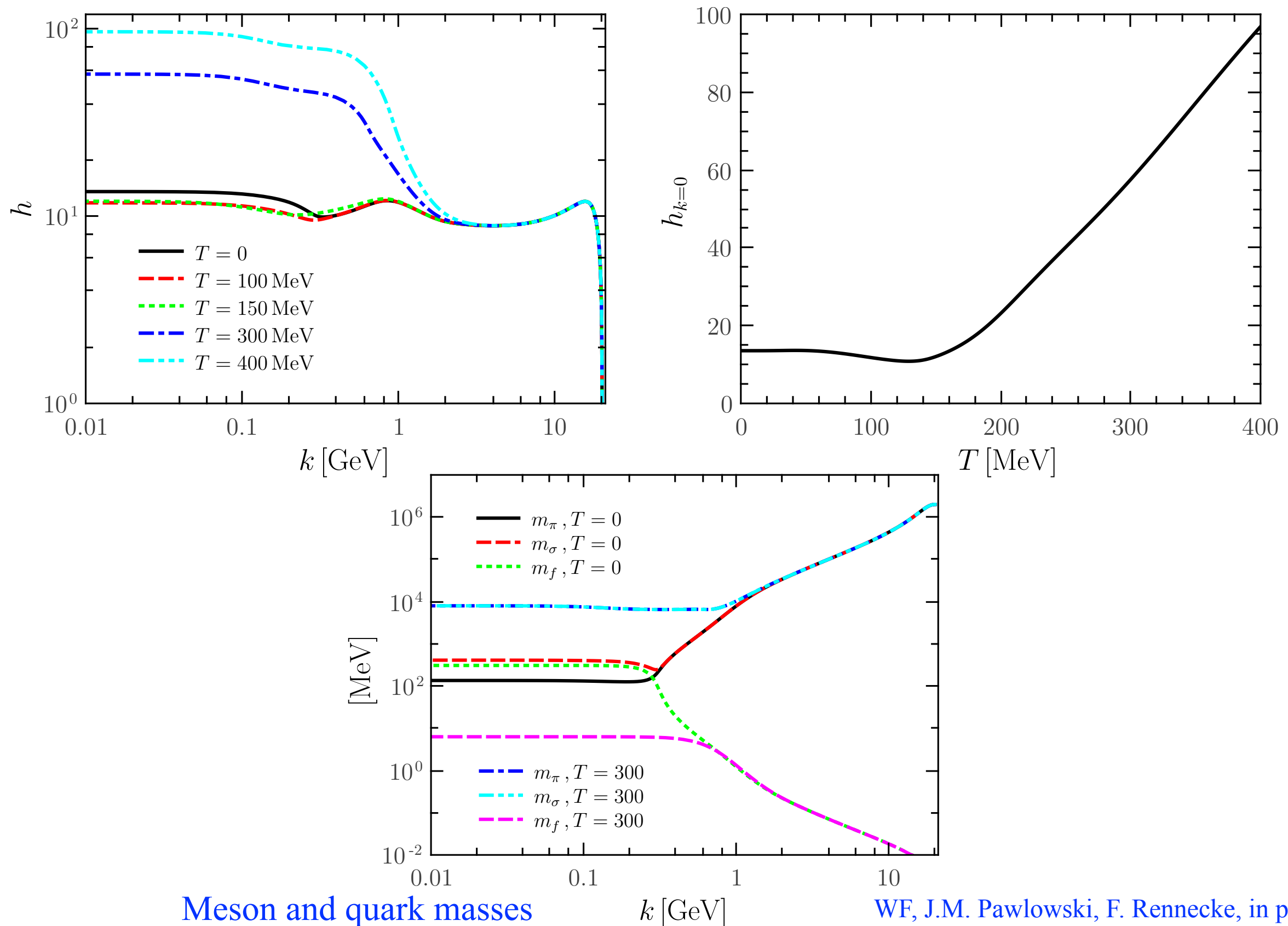
Running of the Strong Coupling



Note only the quark loop for the gluon are included for the moment, thermal effects of gluon loops are in progress.

Gluon dressing function

Yukawa coupling and Masses



Meson and quark masses

WF, J.M. Pawłowski, F. Rennecke, in preparation

Summary and outlook

Summary and outlook

- ★ Baryon number fluctuations and baryon number probability distribution have been investigated in the 2 and 2+1 flavor effective models within the FRG approach.
- ★ Better agreement with lattice simulations and experiments is observed with the improvement of the truncations.
- ★ We have also performed FRG QCD calculations at finite temperature. The QCD phase transitions have been investigated.
- ★ Phase structure and thermodynamics investigated in the FRG QCD approach are in progress.

Summary and outlook

- ★ Baryon number fluctuations and baryon number probability distribution have been investigated in the 2 and 2+1 flavor effective models within the FRG approach.
- ★ Better agreement with lattice simulations and experiments is observed with the improvement of the truncations.
- ★ We have also performed FRG QCD calculations at finite temperature. The QCD phase transitions have been investigated.
- ★ Phase structure and thermodynamics investigated in the FRG QCD approach are in progress.

Thank you very much for your attentions!